Article:
Tao, C.-N., Buswell, W., Zhang, P. et al. (4 more authors) (2022) A single amino acid transporter controls the uptake of priming-inducing beta-amino acids and the associated trade-off between induced resistance and plant growth. Plant Cell. koac271. ISSN 1040-4651

https://doi.org/10.1093/plcell/koac271

RESEARCH ARTICLE

A single amino acid transporter controls the uptake of priming-inducing beta-amino acids and the associated trade-off between induced resistance and plant growth.

Chia-Nan Tao[1], Will Buswell[1], Peijun Zhang[1], Heather Walker[1, 2], Irene Johnson[1], Katie Field[1], Roland Schwarzenbacher[1,3] and Jurriaan Ton[1, a]

[1] School of Biosciences, Institute for Sustainable Food, The University of Sheffield, Sheffield S10 2TN, United Kingdom

[2] *bi*OMICS Facility, Department of Animal and Plant Sciences, University of Sheffield, Sheffield S10 2TN, United Kingdom

[3] Present address: Department of Biosciences, Durham University, Durham, DH1 3LE, United Kingdom

[a] corresponding author: Jurriaan Ton (j.ton@sheffield.ac.uk)

Key Words: BABA, RBH, defense priming agents, amino acid transporter, LHT1, Arabidopsis, defense-growth trade-off.

Short title: The cellular transporter of RBH and BABA

One-sentence summary: A forward genetic screen revealed the transporter of two resistance-inducing beta-amino acids, BABA and RBH, which balance growth and induced resistance

The author(s) responsible for distribution of materials integral to the findings presented in this article in accordance with the policy described in the Instructions for Authors (https://academic.oup.com/plcell/pages/General-Instructions) is: Jurriaan Ton (j.ton@sheffield.ac.uk).

ABSTRACT

Selected beta-amino acids, such as beta-aminobutyric acid (BABA) and R-beta-homoserine (RBH), can prime plants for resistance against a broad spectrum of diseases. Here, we describe a genome-wide screen of fully annotated *Arabidopsis thaliana* T-DNA insertion lines for *impaired in RBH-induced immunity* (*iri*) mutants against the downy mildew pathogen *Hyaloperonospora arabidopsidis*, yielding 104 lines that were partially affected and four lines that were completely impaired in RBH-induced resistance. We confirmed the *iri1-1* mutant phenotype with an independent T-DNA insertion line in the same gene, encoding the high-affinity amino acid transporter LYSINE HISTIDINE TRANSPORTER 1 (LHT1). Uptake experiments with yeast cells expressing *LHT1* and mass spectrometry-based quantification of RBH and BABA in leaves of *lht1* mutant and *LHT1* overexpression lines revealed that LHT1 acts as the main transporter for cellular uptake and systemic distribution of RBH and BABA. Subsequent characterization of *lht1* mutant and *LHT1* overexpression lines for induced resistance and growth responses revealed that the levels of LHT1-mediated uptake determine the trade-off between induced resistance and plant growth by RBH and BABA.

IN A NUTSHELL

Background: Specific chemicals can induce long-lasting disease resistance in plants. These chemicals act by mediating a form of immune memory, called 'priming', which enables the plant to activate a faster and/or stronger defence response upon future pathogen attack. The beta-amino acids beta-aminobutyric acid (BABA) and R-beta-homoserine (RBH) are particularly effective in priming taxonomically unrelated plants against a wide range of diseases. Previous research from our lab has shown that BABA and RBH, despite their structural similarity, are perceived and controlled by different receptors and pathways. However, the transporter responsible for the cellular uptake of these two priming agents has remained unknown.

Question: To identify new genes controlling RBH-induced resistance in Arabidopsis, we carried out a genetic screen for Arabidopsis mutants that are impaired in RBH-induced immunity against the downy mildew pathogen *Hyaloperonospora arabidopsidis* (*Hpa*). The first mutant that we isolated turned out to be affected in the high-affinity amino acid transporter LYSINE HISTIDINE TRANSPORTER 1 (LHT1).

Findings: Experiments to characterize the Arabidopsis *lht1* mutant demonstrated that LHT1 controls resistance induced by RBH and BABA by controlling the uptake of these chemicals from the soil. Competition experiments with the LHT1 substrate L-alanine and yeast cells expressing the *LHT1* gene confirmed that LHT1 acts as a high-affinity transporter of RBH and BABA. Subsequent characterization of mutant and over-expression lines of Arabidopsis

revealed that the uptake level by LHT1 controls not only the resistance response to RBH and BABA, but also the phytotoxic side-effects upon chemical overstimulation with higher concentrations. Hence, LHT1 acts as a master regulator of the trade-off between induced resistance and growth caused by RBH or BABA.

Next steps: An important take home message from our study is that the trade-off between induced resistance and growth by resistance-inducing beta-amino acids like BABA and RBH can be optimized by manipulating the *LHT1* gene. This conclusion offers major translational opportunities for breeding programs that aim to exploit BABA- and/or RBH-induced resistance in crops, but suffer from the phytotoxicity of these agents.

INTRODUCTION

The innate immune system enables plants to perceive and react to attacks by pathogens and herbivores. The basal component of this regulatory system is under the control of pattern recognition receptors (PRRs) that perceive molecular non-self-patterns from the attacker or damaged-self patterns that form during an attack (Choi and Klessig, 2016). Following recognition of these alarm signals, a signaling network is initiated that orchestrates the induction of cellular defense mechanisms, including reactive oxygen species (ROS), callose-rich cell wall depositions and the induction of defense-related genes (Chisholm et al., 2006; Bigeard et al., 2015). Besides this pattern-triggered immunity (PTI), innate immunity can be triggered by susceptibility-inducing pathogen effectors. If the challenged plant expresses a resistance (R) gene that can recognize the activity of such a pathogen effector, the innate immune response is referred to as effector-triggered immunity (ETI; Cui et al., 2015). In addition to innate immunity, plants can acquire long-lasting resistance, which develops after recovery from biotic stress. This induced resistance (IR) is typically based on the priming of the innate immune system, which mediates a faster and/or stronger induction of inducible defenses upon secondary attack (Wilkinson et al., 2019; De Kesel et al., 2021). Moreover, IR can be triggered by root colonization of selected plant beneficial microbes or treatment with specific chemical agents, such as microbe-associated molecular patterns, volatile organic compounds and non-proteinogenic β-amino acids (Mauch-Mani et al., 2017; De Kesel et al., 2021).

β-amino butyric acid-induced resistance (BABA-IR) has emerged as a popular model system to study the molecular mechanisms controlling immune priming in plants. BABA-IR has been reported in more than 40 plant species against different types of pathogens (Cohen, 1994; Cohen et al., 2016). In Arabidopsis (*Arabidopsis thaliana*), BABA primes both salicylic acid (SA) dependent and independent defense mechanisms and protects plants

against biotrophic, hemibiotrophic and necrotrophic pathogens (Zimmerli et al., 2000; Ton et al., 2005; Schwarzenbacher et al., 2020). Recent evidence suggests that BABA accumulates during exposure to biotic and abiotic stress (Thevenet et al., 2017), which provides biological relevance and supports previous evidence that an aspartyl tRNA aspartase, IMPAIRED IN BABA-INDUCED DISEASE IMMUNITY 1 (IBI1), acts as a plant receptor for BABA (Luna et al., 2014). BABA was also suggested to act as a microbial rhizosphere signal, based on the finding that induced systemic resistance (ISR) upon root colonization by *Pseudomonas simiae* WCS417 is blocked in the *ibi1-1* mutant (Luna et al., 2014). Despite the apparently high efficiency by which plant roots are capable of taking up BABA from the soil (Zimmerli et al., 2000; Ton et al., 2005), a cellular transporter for this well-known priming agent has not been identified.

Although BABA-IR is effective against a broad spectrum of plant diseases, high doses of BABA results in major growth reduction (Wu et al., 2010; Luna et al., 2014). This undesirable side effect is partly caused by disruptive binding of R-BABA to the aspartic acid-binding pocket of the IBI1 enzyme, causing the accumulation of uncharged $tRNA^{Asp}$ and GCN2 (GENERAL CONTROL NON-DEREPRESSIBLE 2)-dependent inhibition of translation (Luna et al., 2014; Buswell et al., 2018). To search for less phytotoxic IR analogs of BABA, we previously screened a small library of structurally related β-amino acids for IR activity and phytotoxicity in Arabidopsis. This screen resulted in the identification of R-β-homoserine (RBH), which induces resistance in Arabidopsis and tomato (*Solanum lycopersicum* L.) cultivar Micro-Tom) against biotrophic and necrotrophic pathogens without growth reduction (Buswell et al., 2018). A recent study comparing four IR agents for their effectiveness in strawberry (*Fragaria* × *ananassa*) against *Botrytis cinerea* also identified RBH as the most effective IR agent without negative effects on plant growth (Badmi et al., 2019). Like BABA, RBH primes defense activity of callose-rich papillae, which in Arabidopsis are formed at relatively early stages of infection by the biotrophic oomycete *Hyaloperonospora arabidopsidis (Hpa).* Interestingly, despite its structural similarity to BABA, RBH does not require the IBI1 receptor to induce resistance in Arabidopsis (Buswell et al., 2018). Furthermore, unlike BABA, RBH does not prime salicylic acid (SA)-dependent induction of gene expression but primes camalexin production upon infection by *Hpa* and the expression of jasmonic acid (JA)-dependent defense genes after infection by the necrotrophic fungus *Plectosphaerella cucumerina* (Zimmerli et al., 2000; Ton et al., 2005; Buswell et al., 2018). Hence, RBH-induced resistance (RBH-IR) is controlled by partially distinct pathways

relative to BABA-IR. Importantly, the molecular mechanisms responsible for the uptake and perception of RBH are unknown.

In this study, we conducted a genome-wide screen of Arabidopsis T-DNA insertion mutants for *impaired in RBH-induced immunity* (*iri*) phenotypes against *Hpa*, yielding 104 and four lines that are partially and completely impaired in RBH-IR, respectively. Of the latter, we characterized the *iri1* mutant, which is affected in the high-affinity amino acid transporter LYSINE HISTIDINE TRANSPORTER 1 (LHT1). We provide evidence that the level of LHT1-mediated uptake determines the balance between IR and plant tolerance by RBH and BABA. Furthermore, mass spectrometry analysis of leaves from RBH- and BABA-treated wild-type, *lht1* mutant and *LHT1*-overexpressing plants revealed that LHT1 is critical for the uptake and systemic distribution of both RBH and BABA, while uptake experiments with *LHT1*-expressing yeast cells demonstrated that LHT1 acts as a high-affinity transporter of BABA and RBH. In support of other studies that have linked LHT1 to plant-microbe interactions and plant immunity, we conclude that LHT1 acts as a master regulator of the trade-off between growth and IR by priming-inducing beta-amino acids.

RESULTS

Genome-wide screen for *impaired in RBH-immunity* (*iri*) mutants

To search for new regulatory genes of RBH-induced resistance, we screened 23,547 T-DNA insertion lines from the SALK and SAIL collections (Alonso and Ecker, 2006) for an *impaired in RBH-induced immunity* (*iri*) phenotype against *Hpa*. This set of T-DNA insertion lines covers >90% of all annotated protein-coding genes in the Arabidopsis genome. In contrast to conventional ethyl methanesulfonate (EMS)-based mutant screens, which rely on the selection of mutant phenotypes in individual plants, the collection of fully annotated homozygous T-DNA insertion mutants allowed us to screen five genetically identical seedlings per line for quantification of the *iri* mutant phenotype, including partial loss of RBH-IR. To reduce false positives, we performed the screen in three successive stages. In the first stage, we screened seedlings in 400-well trays, in which the soil was soaked to saturation with RBH to a final soil concentration of ~0.5 mM, followed by inoculation with *Hpa* conidiospores and scoring for visual sporulation at 5-7 days post inoculation (dpi; Figure 1A). Each tray yielded ~1-2 lines displaying sporulation for at least two seedlings/well by 7 dpi; these lines were selected and rescreened during stage 2, using the same 400-well tray

selection system. Stage 2 yielded 427 putative *iri* mutant lines (Figure 1A). These putative *iri* mutant lines were taken forward for final validation in stage 3, which was based on categorical scoring of *Hpa* colonization in trypan-blue-stained leaves from control- and RBH-treated plants (0.5 mM) of each candidate line (Figure 1A). To validate the statistical robustness of this screening stage, we conducted a pilot experiment that compared *Hpa* colonization between 40 pots of Col-0 seedlings pre-treated with either water or RBH (0.5 mM). Categorical scoring of trypan blue-stained leaves confirmed statistically uniform distributions of *Hpa* colonization within each treatment (Supplemental Figure 1A). Of the 427 putative *iri* lines from stage 2, we confirmed 104 lines as having partially impaired RBH-IR in stage 3, as evidenced by statistically enhanced levels of *Hpa* colonization in RBH-treated mutant plants compared to RBH-treated wild-type plants, while still showing a statistically significant reduction in *Hpa* colonization by RBH treatment compared to the water controls (Figure 1A, Supplemental Figure S1B and Supplemental Data Set S1). An additional four lines, named *iri1-1* to *iri4-1*, showed a full impairment of RBH-IR, as indicated by statistically identical levels of *Hpa* colonization between RBH- and water-treated plants within each line (Figure 1A, Supplemental Figure S1B and Supplemental Data Set S1).

Identification of *IRI1/LHT1* as a critical regulator of RBH-IR against *Hpa*

Since SALK/SAIL lines can carry multiple T-DNA insertions and/or T-DNA-induced mutations (Alonso and Ecker, 2006), it is possible that the *iri* mutant phenotypes are caused by mutations in genes other than those identified and annotated by PCR border recovery analysis. To address this possibility, we quantified RBH-IR in independent T-DNA insertion lines in the annotated genes for each of the four complete *iri* lines (Figure 1B,C and Supplemental Figure S2A,B). Since RBH-IR against *Hpa* in Arabidopsis is associated with greater effectiveness of callose-rich papillae (Buswell et al., 2018), we quantified the effectiveness of callose-mediated cell wall defense at 3 dpi, as detailed previously (Schwarzenbacher et al., 2020). All original *iri* lines consistently lacked RBH-IR and concomitantly failed to augment callose-mediated defense upon RBH treatment (Figure 1D, Supplemental Figure 2C), confirming the importance of this post-invasive defense barrier in RBH-IR against *Hpa*. However, independent T-DNA insertions in the annotated genes inactivated in *iri2-1*, *iri3-1* or *iri4-1* did not affect RBH-IR and showed wild-type levels of

callose-mediated defense against *Hpa* (Supplemental Figure 2C), indicating that their *iri* phenotypes are caused by T-DNA-induced mutations in other genes. By contrast, an independent T-DNA insertion mutant (*iri1-2*) in the annotated gene disrupted in *iri1-1* displayed a complete *iri* phenotype (Figures 1B and 1C) and was concomitantly impaired in RBH-induced priming of callose defense (Figure 1D). The *iri1-1* and *iri1-2* mutants carry a T-DNA insertion in the 5th intron and the 2nd intron of *LYSINE HISTIDINE TRANSPORTER1* (*LHT1*; At5g40780; Figure 1B; Supplemental Figures S3A and S3B), respectively. *LHT1* encodes a high-affinity amino acid transporter for acidic and neutral amino acids in roots and mesophyll cells (Chen and Bush, 1997; Hirner et al., 2006; Svennerstam et al., 2007). We will therefore refer to *IRI1* as *LHT1* thereafter.

LHT1 controls RBH uptake from the soil.

Since LHT1 was characterized as an amino acid transporter (Chen and Bush, 1997), we hypothesized that the lack of RBH-IR in *lht1* mutants (*lht1-5*, for *iri1-1*; and *lht1-4*, for *iri1-2*) might be caused by impaired RBH uptake from the soil. To test this hypothesis, we determined RBH concentrations after saturating the soil with increasing RBH concentrations in the leaves of Col-0, *iri1-1* and a previously characterized *LHT1* overexpression line (Hirner et al., 2006; *35Spro:LHT1*), which shows a 27-fold higher *LHT1* expression level than Col-0 plants under our experimental conditions (Supplemental Figure S3C). At 2 days after soil treatment, we harvested replicate leaf tissues for RBH quantification by hydrophilic interaction liquid chromatography coupled to quadrupole time-of-flight mass spectrometry (HILIC-Q-TOF; Figure 2A) or challenged the leaves with *Hpa* to quantify RBH-IR (Figure 2B). The three genotypes differed statistically in their RBH shoot concentrations after soil treatment with increasing RBH concentrations, as evidenced by a highly statically significant interaction between soil treatment and genotype (two-way ANOVA; $p<0.001$; Figure 2A). For both Col-0 and *35Spro:LHT1,* RBH shoot accumulation showed a dose-dependent rise with increasing RBH concentrations in the soil. The *35Spro:LHT1* seedlings accumulated statistically higher RBH concentrations in their shoots than Col-0 after saturating the soil to a final concentration of 0.15 mM or 0.5 mM RBH, whereas RBH concentrations in the shoot of *lht1-5* were hardly detectable by HILIC-Q-TOF and failed to show a dose-dependent increase with RBH soil treatment (Figure 2A). The observed variation in RBH shoot concentrations correlated with RBH-IR intensity against *Hpa* (Figure 2B); while RBH failed to induce

229 statistically significant levels of resistance in *lht1-5* at all concentration tested, *35Spro:LHT1*
230 plants showed increased levels of RBH-IR compared to Col-0 at all RBH concentrations
231 tested. Notably, the relatively low concentration of 0.05 mM RBH failed to protect Col-0
232 against *Hpa* seedlings, whereas the same RBH concentration induced a statistically
233 significant reduction in *Hpa* colonization in *35Spro:LHT1* (Figure 2B). Thus, RBH uptake
234 from the soil by LHT1 increases by overexpression of *LHT1*, which in turn boosts RBH-IR
235 against *Hpa*.

236

237 **Tolerance to RBH depends on LHT and not on catabolism**

238 In contrast to BABA, RBH induces resistance in Arabidopsis without concomitant growth
239 inhibition (Buswell et al., 2018). To examine whether LHT1 controls tolerance to RBH, we
240 quantified seedling growth of Col-0, *lht1-5*, and *35Spro:LHT1* on Murashige and Skoog (MS)
241 agar medium. To strengthen the evidence that RBH-induced phytotoxicity in *35Spro:LHT1*
242 depends on LHT1 uptake, we conducted this experiment in the presence of increasing
243 concentrations of L-Ala, a high-affinity substrate of LHT1 (Hirner et al., 2006), expecting
244 that if tolerance is controlled by LHT1-dependent uptake, the L-Ala in the medium would
245 outcompete RBH for uptake and antagonize RBH-induced phytotoxicity. Indeed, while green
246 leaf areas (GLA) of Col-0 and *lht1-5* were unaffected by increasing concentrations of RBH
247 after 1 week of growth, growth of the *35Spro:LHT1* overexpression line showed a dose-
248 dependent repression with increasing RBH concentrations, which was antagonized by L-Ala
249 in a dose-dependent manner (Figure 3). Together with our earlier finding that RBH uptake
250 increased in the *35Spro:LHT1* line (Figure 2A), these results indicate that natural tolerance of
251 Arabidopsis to RBH (Buswell et al., 2018) is determined by RBH uptake capacity of LHT1.

252 To exclude a role for catabolism in RBH tolerance, we repeated the experiment on
253 MS medium without inorganic nitrogen (N_{inorg}; NO_3^- and NH_4^+), supplemented with
254 increasing concentrations of RBH and L-Ala. Importantly, Arabidopsis failed to grow on agar
255 medium without N_{inorg} (Supplemental Figure S4), and increasing RBH concentrations in the
256 growth medium failed to rescue growth. Hence, Arabidopsis cannot metabolize RBH as a N
257 source, which rules out metabolic breakdown (catabolism) as a mechanism of RBH tolerance.
258 By contrast, increasing L-Ala concentrations added to the agar medium rescued seedling
259 growth of all genotypes, albeit to varying degrees. While *35Spro:LHT1* seedlings showed the
260 strongest growth response to increasing L-Ala concentrations, Col-0 displayed an

intermediate growth response, followed by a relatively weak growth response in *lht1-5* (Supplemental Figure S4), thus confirming the contribution of LHT1 to L-Ala uptake (Hirner et al., 2006; Svennerstam et al., 2007; Svennerstam et al., 2011). Notably, increasing RBH concentrations in the presence of L-Ala caused a dose-dependent growth reduction in *35Spro:LHT1* seedlings but not in Col-0 or *lht1-5* (Supplemental Figure S4), which supports our conclusion that increased RBH uptake through *LHT1* overexpression renders Arabidopsis sensitive to RBH-induced stress due to accumulation of phytotoxic RBH concentrations that cannot be catabolized. Thus, tolerance of Arabidopsis to RBH is controlled by LHT1-dependent uptake of RBH, rather than catabolism of RBH.

LHT1 also controls BABA uptake, BABA-IR and BABA tolerance.

Given the published broad substrate range of the LHT1 transporter for acidic and neutral amino acids (Hirner et al., 2006; Svennerstam et al., 2007), we examined whether LHT1 also plays a role in the uptake of BABA. To this end, we harvested replicate shoot tissues of Col-0 and *lht1-5* seedlings to quantify *in planta* concentrations of BABA at 2 days after saturating the soil with increasing concentrations of the chemical (0, 0.025, 0.05, 0.15 and 0.5 mM), using HILIC-Q-TOF (Figure 4A). While saturating the soil on which Col-0 seedlings grew with increasing BABA concentrations resulted in a dose-dependent increase of BABA concentrations in the shoot (Figure 4A), a similar treatment of the *lht1-5* mutant failed to increase shoot BABA concentrations (Figure 4A), indicating that BABA uptake is dependent on LHT1. To corroborate this, we saturated the soil of Col-0, *lht1-5* and *35Spro:LHT1* seedlings with increasing BABA concentrations and scored BABA-IR against *Hpa* (Figure 4B). As reported previously, BABA was more efficient than RBH in protecting Col-0 against *Hpa* (Buswell et al., 2018), already reducing *Hpa* colonization at 0.025 mM BABA and reaching maximum levels of resistance at concentrations of 0.05 mM and higher (Figure 4B). The *35Spro:LHT1* line showed even higher levels of resistance at 0.025 mM BABA compared to Col-0, indicating that these seedlings are sensitized to respond to BABA. By contrast, the *lht1-5* mutant was severely compromised in its effectiveness of BABA-IR, and only displayed weak levels of IR at soil BABA concentrations of 0.25 mM and 0.5 mM (Figure 4B). Thus, like RBH-IR, BABA-IR depends on a functional LHT1 transporter and is enhanced by overexpression of *LHT1*.

To determine whether LHT1 also controls BABA-induced phytotoxicity, we quantified the growth of Col-0, *lht1-5* and *35Spro:LHT1* seedlings growing on MS agar plates supplemented with phytotoxic concentrations of BABA. As shown in Figure 5, GLA values of Col-0 after 1 week of growth declined with increasing BABA concentrations. This BABA-induced stress increased dramatically in *35Spro:LHT1* seedlings and decreased in *lht1-5* seedlings (Figure 5). The fact that *lht1-5* seedlings still showed growth repression at higher BABA concentrations suggests that additional mechanisms contribute to BABA-induced phytotoxicity. To compare the severity of RBH- and BABA-induced phytotoxicity, we cultivated Col-0, *lht1-5* and *35Spro:LHT1* seedlings on MS agar plates containing the same doses of RBH or BABA (0.25 mM, 0.5 mM, 1 mM or 2.5 mM). Of the three genotypes tested, only *35Spro:LHT1* seedlings were affected in growth by both chemicals at concentrations of 0.25 mM and above (Supplemental Figure S5A), with BABA causing more severe growth repression than RBH (Supplemental Figure S5B). Quantification of green leaf areas of *35Spro:LHT1* across all inhibitor concentrations confirmed that BABA is more potent in repressing growth than RBH (Supplemental Figure S5B). Collectively, our results indicate that LHT1 is the dominant transporter for BABA uptake from the soil, controlling both BABA-IR and BABA-induced stress.

LHT1 transports both RBH and BABA

Having established that LHT1 is responsible for the uptake of RBH and BABA, we next examined the kinetics by which LHT1 transports these β-amino acids. To this end, we heterologously expressed the Arabidopsis *LHT1* coding sequence in the yeast (*Saccharomyces cerevisiae*) 22Δ10α strain, which lacks ten amino acid transporter genes and is completely deficient in the uptake of amino acids (Besnard et al., 2016). In contrast to empty vector (EV)-transformed 22Δ10α cells, the *LHT1*-expressing 22Δ10α strain was capable of growing on agar plates containing 1 mM L-Ala as the only nitrogen (N) source (Figure 6A), while supplementing liquid growth medium without inorganic $(NH_4)_2SO_4$ with increasing L-Ala concentrations steadily improved planktonic growth by *LHT1*-expressing 22Δ10α cells (Figure 6B). Increasing RBH and BABA concentrations in liquid growth medium with 1 mM L-ala repressed growth by *LHT1*-expressing 22Δ10α cells completely (Supplemental Figures S6A and S6B, respectively), despite the fact that both chemicals only marginally repressed 22Δ10α growth in liquid medium with 10 mM $(NH_4)_2SO_4$ as an N

source (Supplemental Figure S7). These results not only show that yeast fails to metabolize RBH and BABA, but they also suggest that increasing RBH and BABA concentrations outcompete L-Ala for cellular uptake.

To study the kinetics of RBH and BABA uptake, we carried out experiments with ^{14}C-labeled L-Ala in the absence and presence of RBH or BABA. To this end, we incubated EV- and *LHT1*-expressing 22Δ10α cells for 2, 5 and 10 min in buffer containing 50 µM or 500 µM L-Ala with a fixed amount of ^{14}C-L-Ala for incubation, after which we quantified cellular L-Ala uptake by ^{14}C scintillation. In contrast to EV-transformed cells, *LHT1*-expressing cells showed a linear uptake for L-Ala over time (Supplemental Figure S8), confirming the functionality of the transporter in yeast. To determine whether RBH and BABA competitively inhibit the LHT1 transporter for L-Ala uptake, we incubated *LHT1*-expressing cells for 5 min in buffer containing increasing concentrations L-Ala and a fixed amount of ^{14}C- L-Ala in the presence or absence of 500 µM RBH or 500 µM BABA (Figure 6C, D). Plotting the uptake velocity (V_{uptake}; fmol L-Ala/cell) against L-Ala concentration revealed a dose-dependent increase until saturation (V_{max}; Figure 6C, D). Based on these data, we calculated that LHT1 has a Km value of 9.4 µM for L-Ala-uptake, which is in line with previously reported Km values for acidic and neutral amino acids (Hirner et al., 2006). Although V_{uptake} in the presence of either 500 µM RBH or 500 µM BABA decreased across a lower range L-Ala concentration, it still reached similar V_{max} values at higher L-Ala concentrations, indicating that RBH and BABA are competitive inhibitors of L-Ala uptake by LHT1. To calculate the inhibition constants (Ki) of RBH and BABA, we conducted further uptake experiments in the presence of multiple inhibitor concentrations (0, 250, and 1,000 µM RBH/BABA) and increasing L-Ala concentrations. We generated Dixon plots of the inverse uptake velocity ($1/V_{uptake}$) against inhibitor concentration (Cornish-Bowden, 1974; Yoshino & Murakami, 2009) to determine Ki values at the intersecting lines of the different L-Ala concentrations (1, 5, 25, 50, 250 µM; Figure 6E,F). Predicted intersects were called at modeled RBH/BABA concentrations that had the smallest $1/V_{uptake}$ range between the various L-Ala concentrations (Supplemental Figure S9), revealing a Ki of 87.9 µM for RBH and a Ki of 68.9 µM for BABA (Figure 6E, F). Hence, LHT1 is a transporter of both beta-amino acids and shows a higher affinity for BABA than for RBH.

DISCUSSION

Using annotated T-DNA insertion lines for a genome-saturating mutant screen

We used a genome-covering collection of Arabidopsis T-DNA insertion lines in a forward mutant screen for regulatory genes of IR. The availability of homozygous T-DNA insertions with high genomic coverage (Alonso and Ecker, 2006) facilitates a near genome-saturating screen. The use of this resource has several benefits compared to conventional mutant screens. First, the availability of T-DNA flanking sequences mapped to the Arabidopsis genome allows for immediate identification of gene candidates without having to commit to a time-consuming generation of mapping populations and linkage analysis. Second, the collection of homozygous mutant lines enables the screening of small populations that all carry the same mutant allele, which facilitates the identification of partial (leaky) mutant phenotypes, as illustrated by the identification of 104 *iri* lines that are partially affected in RBH-IR (Figure 1A; Supplemental Figure S1, Supplemental Data Set S1). This relatively high number of partial *iri* mutants supports the notion that IR is a highly quantitative form of resistance, relying on the additive contribution of multiple genes (Ton et al. 2006; Ahmad et al. 2010, Wilkinson et al. 2019). Thus, the within-genotype replication of this screen enables selection for genes that make a quantitative contribution to complex multigenic traits. A disadvantage of using annotated T-DNA insertion lines in a forward mutant screen is that a single T-DNA insertion line can carry multiple mutations (O'Malley et al., 2015). These mutations are not necessarily covered by the annotated T-DNA flanking sequences, since they can be caused by truncated T-DNA elements or mis-repairs of integration sites from abortive T-DNA integrations (leaving mutational footprints; Gelvin, 2021). Indeed, several other studies have reported that mutant phenotypes in this collection of T-DNA insertion lines do not always co-segregate with the annotated T-DNA insertion (De Muyt et al., 2009; Dobritsa et al., 2011; Wilson-Sánchez et al., 2014). To account for this issue, we validated the mutant phenotypes of the four complete *iri* mutants in independent T-DNA insertion lines of their disrupted annotated genes for both RBH-IR and augmented cell wall defense against *Hpa* (Figure 1C, 1D and Supplemental Figure S2). Even though the *iri* phenotypes of the four original mutant lines were robust and reproducible (Figure 1C, D and Supplemental Figure S2), only the phenotype of the *lht1-5* (*iri1-1*) mutant could be confirmed in an independent T-DNA insertion line in the annotated disrupted gene. Identifying the causal mutation in the other three *iri* lines will require thermal asymmetric interlaced PCR (TAIL-PCR) to identify flanking sequences of alternative T-DNA insertions or conventional linkage analysis in segregating mapping populations.

The role of LHT1 in plant-biotic interactions

IRI1 encodes the broad-range amino acid transporter LHT1. Cellular transporters play important roles in the control of plant-pathogen interactions by facilitating pathogen feeding (Elashry et al., 2013; Marella et al., 2013), secretion of antibiotic compounds (Lu et al., 2015; Khare et al., 2017), transporting defense plant hormones (Serrano et al., 2013), or contributing to plant defense responses (Liu et al., 2010; Yang et al., 2014). Furthermore, the *LHT1* ortholog *LjLHT1.2* in birdsfoot trefoil (*Lotus japonicus*) is transcriptionally induced by arbuscular mycorrhizal fungi (AMF; Guether et al., 2011), suggesting that it facilitates AMF-dependent uptake of organic nitrogen. Given the role of LHT1 in IR, it is tempting to speculate that LHT1 also plays a role in mycorrhiza-IR (Cameron et al., 2013). In Arabidopsis. LHT1 has been implicated in the direct regulation of SA-dependent disease resistance. Liu et al. (2010) reported that *lht1* mutant lines had increased basal resistance against the hemibiotrophic bacterium *Pseudomonas syringae* pv. *tomato*, the hemibiotrophic fungus *Colletotrichum higginsianum*, and the biotrophic fungus *Erysiphe cichoracearum*. The study furthermore provided evidence that LHT1 controls plant immunity by cellular uptake of L-glutamine (L-Gln), which is a precursor of the redox-buffering compound glutathione. Liu et al. (2010) proposed that the lower L-Gln uptake capacity in *lht1* mutants suppresses cellular redox buffering capacity, thereby enabling augmented elicitation of ROS and SA-dependent defenses upon pathogen attack. Our experiments did not reveal statistically significant differences in basal defense against the biotrophic oomycete *Hpa* between wild-type and *lht1* mutant plants (Figures 1 and 2), in contrast to the results shown by Liu et al. (2010). This discrepancy may be explained by the fact that we used relatively young plants (2- to 3-week-old seedlings), which do not express SA-dependent age-related resistance (ARR; Kus et al., 2002). Indeed, other studies have reported that *lht1* seedlings display normal growth phenotypes without the enhanced SA levels observed in older plants (Liu et al., 2010; Zhang et al., 2022). Accordingly, it is possible that glutamine-dependent redox regulation contributes to age-related resistance in older plants. Since *LHT1* expression is lower in seedlings (Hirner et al., 2006), it is also possible that other amino transporters contribute to the cellular delivery of glutamine in these younger seedlings, such as AMINO ACID PERMEASE 1 (AAP1; Boorer et al., 1996) or CATIONIC AMINO ACID TRANSPORTER 8 (CAT8; Yang et al., 2010). Interestingly, in contrast to the negative role of LHT1 in innate immunity reported by Liu et al. (2010), a recent study by Yoo et al. (2020)

422 revealed that LHT1 contributes positively to ETI-related resistance in Arabidopsis against
423 *Pseudomonas syringae* pv. *maculicola* carrying the avirulence gene *AvrRpt2*. Moreover,
424 Zhang et al. (2022) showed that LHT1 is the dominant transporter responsible for increased
425 amino acid uptake during early PTI against pathogenic *Pseudomonas syringae*, when it has a
426 positive contribution to resistance by restricting bacterial colonization. Hence, LHT1 has
427 been reported to have both positive and negative roles in innate plant resistance. It should be
428 noted, however, that the immune-related function of LHT1 described in our study is related to
429 IR by priming-inducing β-amino acids, rather than innate resistance.

430

431 **The role of LHT1 in beta-amino acid-IR**

432 Our results have shown that LHT1 is the dominant transporter for cellular uptake of RBH and
433 BABA from the soil (Figures 2 and 4). LHT1 localizes to the cell membrane (Hirner et al.,
434 2006), which enables cellular import of RBH and BABA from the apoplast. *LHT1* is
435 expressed in root tips, lateral roots and mature leaves (Hirner et al., 2006), enabling cellular
436 uptake of RBH and BABA in both roots and leaves. Since *LHT1* is not expressed in the leaf
437 vein, we propose that the activity of RBH and BABA in leaves is preceded by long-distance
438 transport via the xylem and apoplastic distribution in the leaves. While BABA was applied
439 exogenously in our experiments, recent studies have reported that biotic and abiotic stresses
440 can elicit low concentrations of endogenous BABA in Arabidopsis (Thevenet et al., 2017;
441 Balmer et al., 2019). Under these conditions, BABA only accumulates in locally stressed
442 tissues and not systemically in non-stressed tissues (Balmer et al., 2019), indicating that
443 stress-induced accumulation of BABA does not contribute to systemic defense signaling.
444 Although the biosynthesis pathway of stress-induced BABA remains unknown, it seems
445 plausible that this local biosynthesis occurs inside the cell. The Ki values of RBH (87.9 µM)
446 and BABA (68.9 µM) indicate that these beta amino acids have marginally lower affinities
447 for LHT1 than endogenous alpha-amino acids (Hirner et al., 2006). Since alpha-amino acids
448 typically reach apoplastic concentrations between 1 µM to 10 µM (Zhang et al., 2022), it
449 would be difficult for BABA to compete with these substrates. Moreover, *Hpa*-induced
450 BABA concentrations do not exceed 25 ng/g fresh weight (242.7 nM; Thevenet et al. 2017),
451 which seems too low to be a competitive substrate for LHT1. Hence, cellular uptake of
452 BABA by LHT1 does not appear to play a major role in *Hpa*-induced BABA accumulation,
453 which would also explain why the *lht1* mutant and *35Spro:LHT1* overexpression lines were

not majorly affected in basal resistance to *Hpa* (Figure 2). Nevertheless, we cannot exclude that *Hpa* locally induces much higher BABA concentrations in the cells directly interacting with the parasite, and that LHT1 plays a role in countering diffusion of this intracellular BABA into the apoplast. In this context, it is interesting to note that *Hpa* infection induces *LHT1* expression (Sonawala et al. 2018; Supplemental Figure S10), which could play a role in upholding defense-inducing intracellular concentrations of BABA in *Hpa*-challenged cells and would also explain why stress-induced BABA is not distributed systemically (Balmer et al. 2019).

While our results provide strong evidence that LHT1 is the dominant transporter for the uptake of RBH and BABA (Figures 2-6), they do not necessarily mean that the contribution of LHT1 to RBH-IR or BABA-IR solely depends on its uptake activity. For instance, while treatment with 0.05 mM RBH resulted in similar foliar concentrations in both *35Spro:LHT1* and wild-type plants (Figure 2A), this relatively low RBH concentration only triggered a significant IR response in *35Spro:LHT1* plants and not in wild-type plants. This uncoupling of RBH concentration from IR suggests that the function of LHT1 in RBH-IR may involve an additional defense signaling activity that becomes active at low RBH concentrations. Such a transporter-receptor co-functionality (transceptor activity) has been reported for NITRATE TRANSPORTER 1.1 (NRT1.1) for nitrate uptake and signaling. Replacing Pro-492 with Leu-492 in NRT1.1 disabled the nitrate transport activity of this protein but not its ability to induce *NRT2.1* expression (Ho et al., 2009), which is a nitrate-responsive gene that has concomitantly been linked to the regulation of disease resistance (Camanes et al., 2012). Although no amino acid transporters have been reported with receptor co-functionality (Dinkeloo et al., 2018), it is tempting to speculate that LHT1 might act as a transceptor of β-amino acids. Site-directed mutagenesis of LHT1 and testing whether its RBH and BABA transport activity can be uncoupled from its role in RBH-IR and BABA-IR would be required to test this attractive hypothesis.

Since the *lht1* mutant still displayed residual levels of BABA-IR and BABA-induced stress after treatment with high BABA doses (Figures 4B, 5B), we cannot exclude the possibility that other amino acid transporters have a minor contribution to BABA uptake. A recent study reported that LHT2 has a similar substrate specificity as LHT1, including several D-amino acids and 1-aminocyclopropane-1-carboxylate (ACC) (Choi et al., 2019), and could thus have a complementary contribution to BABA uptake.

RBH and BABA compete with proteinogenic amino acids for uptake by LHT1

We used *LHT1*-expressing yeast cells to assess competitive inhibition of L-Ala uptake by RBH and BABA. Our uptake essays revealed a Km for LHT1 of 9.4 μM for L-Ala (Figure 6C), which supports previously reported Km values of LHT1 for proteinogenic amino acids (Hirner et al., 2006). Furthermore, the inhibitory kinetics of RBH or BABA on L-Ala uptake confirmed competitive inhibition, as evidenced by the fact that L-Ala uptake in the presence of RBH or BABA still reached maximum velocities at higher L-Ala concentrations (Figure 6C,D). Of the two beta-amino acids, BABA had a lower Ki than RBH (68.9 μM vs 87.9 μM), suggesting that LHT1 has a higher affinity for BABA than RBH (Figure 6E,F). This difference in affinity is consistent with our observation that BABA has a stronger inhibitory effect on growth of *35Spro:LHT1* than RBH (Supplemental Figure 5). Since the affinity of LHT1 has been reported to be similar or higher for a range of acidic and neutral amino acids, including L-Gln (Hirner et al., 2006; Svennerstam et al., 2007), our results also explain previous findings by Wu et al. (2010), who showed that BABA-induced phytotoxicity in Arabidopsis can be alleviated by co-application with L-Gln.

LHT1: not just a transporter for proteinogenic amino acids

Although LHT1 was initially identified as a transporter for proteinogenic amino acids (Chen and Bush, 1997), subsequent studies have shown that it transports a much wider range for non-proteinogenic amino acids, such as the ethylene precursor ACC (Shin et al., 2015) and xenobiotic amino acid conjugates (Chen et al., 2018; Jiang et al., 2018). Consistent with this broad-spectrum uptake activity, we showed that LHT1 is the main transporter of the β-amino acids RBH and BABA. Of particular interest is the regulatory function of LHT1 in the trade-off between beta-amino acid-IR and plant growth. For BABA, overexpression of *LHT1* in Arabidopsis increased BABA-IR at the relatively low concentration of 0.025 mM BABA (Figure 4) but it also dramatically increased plant sensitivity to BABA-induced growth repression (Figure 5 and Supplemental Figure S5). However, RBH elicited high levels of IR in wild-type plants at soil concentrations of 0.15 mM RBH and above (Figure 2B) but did not repress growth across all concentrations tested (Figure 3), supporting our earlier conclusion that RBH induces disease resistance without costs on plant growth (Buswell et al. 2018). Interestingly, *35Spro:LHT1* overexpression plants increased the level of IR at relatively low

RBH concentrations (Figure 2B), but also repressed growth in a dose-dependent manner (Figure 3 and Supplemental Figure 5). Direct comparison of RBH- and BABA-induced growth repression in *35Spro:LHT1* plants confirmed that BABA is more active than RBH (Supplemental Figure S5B), which is also apparent from the IR response (Figures 2B, 4B). It is worth noting that the molecular mechanisms of RBH-induced stress remain unclear, and its lower toxicity in plants might come from a combination of uptake and intracellular modes of action.

The observed trade-offs between beta-amino acid-IR and plant growth reveal two important conclusions. First, like BABA, RBH can repress plant growth, but this phytotoxicity depends on LHT1-dependent uptake capacity rather RBH catabolism. Second, our results show that the trade-off between beta-amino acid-IR and growth can be optimized in favor of the IR response by manipulating the *LHT1* gene. This conclusion holds major translational value for breeding programs aiming to exploit BABA-IR in vegetable crops that are protected by BABA but also suffer from BABA-induced phytotoxicity (Cohen et al., 2016; Yassin et al., 2021).

MATERIALS AND METHODS

Biological material

All Arabidopsis (*Arabidopsis thaliana*) genotypes were in accession Columbia-0 (Col-0). The *iri1-1* mutant (*lht1-5*l) and *iri1-2* mutant (*lht1-4*) were described previously by Svennerstam et al. (2007) and Liu et al. (2010); the *35Spro: LHT1* overexpression lines were described by Hirner et al. (2006). The *iri* mutant screen was performed with fully annotated T-DNA insertion lines from the SALK and SAIL collections (Alonso *et al.*, 2003) and purchased from the Nottingham Arabidopsis Stock Centre (sets N27941, N27951, N27942, N27943, N27944, N27945). The annotated T-DNA insertions in *iri1-1* (SALK_115555), *iri1-2* (SALK_036871), *iri2-1* (SALK_204380), SAIL_902_B08, *iri3-1* (SALK_118654), SALK_078838, *iri4-1* (SALK_076708) and SALK_046376 were confirmed by PCR before further testing (Supplemental Table S1), as described below. *Hyaloperonospora arabidopsidis* strain WACO9 was maintained in its asexual cycle by alternate conidiospore inoculations of Col-0 and Ws NahG plants.

549 **Plant growth conditions**

550 For soil-based IR experiments, seeds were sown in a 2:1 (v/v) Scott's Levington M3
551 compost/sand mixture and stratified for 2-4 days in the dark at 4°C. Plants were subsequently
552 cultivated under short-day conditions (8-h light (Sylvania GroLux T8 36W or Valoya NS1
553 LED); 150 µmol photons m^{-2} s^{-1}; 21°C; and 16-h dark; 18°C) with a ~60% relative humidity
554 (RH). Plants for seed propagation were grown in long-day growth conditions (16-h light
555 (Sylvania GroLux T8 36W); 150 µmol photons m^{-2} s^{-1}; 21°C; and 8-h dark; 18°C) with
556 ~60% RH. For plate assays, seeds were surface sterilized (vapor-phase sterilization method)
557 prior to sowing on half-strength Murashige and Skoog (MS) medium (pH = 5.7 and 1%
558 sucrose), solidified with 1.5% (w/v).

559 **Mutant screen**

560 Approximately 10-15 seeds for each seed line were sown in individual wells of 400-well
561 trays (Teku JP 3050/230 H). Each tray was filled with ~2.4 L of compost/sand mixture. After
562 sowing, stratification of seeds and seed germination, seedlings were thinned to five
563 seedlings/well. Two-week-old seedlings were treated with RBH by watering each tray with
564 1.5 L of 2x concentrated RBH solution (1 mM), which was left overnight to saturate the soil.
565 Excess RBH solution (~300 mL) was removed the next morning, resulting in a final soil
566 concentration of ~0.5 mM RBH. Challenge inoculation was performed at 2 days after RBH
567 treatment by spraying seedlings with a suspension of *Hpa* conidiospores (10^5 spores/mL).
568 Trays were sealed with clingfilm after inoculation to maintain 100% RH and promote
569 infection. To verify RBH-IR, each tray contained three randomly distributed wells with Col-0
570 seedlings. Furthermore, to verify favorable conditions for *Hpa* disease, three additional wells
571 with Col-0 seedlings were cut out from each tray and left outside during RBH-uptake to
572 prevent RBH-IR prior to inoculation. At 5-7 dpi, trays were visually inspected for *Hpa*
573 sporulation when sporulation on Col-0 seedlings in the untreated wells of the tray became
574 apparent. Lines developing sporulation within 7 dpi were scored as stage 1 *impaired in RBH-*
575 *induced-immunity* (S1 *iri*) lines, while nongerminated lines were scored as stage 1
576 nongerminated (S1 *ug*). All S1 *iri* and S1 *ug* lines were pooled for the stage 2 screen in 400-
577 well trays, as described above. S1 *iri* lines allowing visible sporulation in two screens time
578 were scored as Stage 2 *iri* (S2 *iri*). S1 *ug* lines that germinated upon rescreening and showed
579 sporulation were re-tested for S2 *iri* phenotypes. Of the 26,631 T-DNA insertion lines,
580 23,547 lines germinated and could be screened for *iri* mutant phenotypes. The 427 putative

iri1 lines selected after stage 2 were pooled for seed bulking and validated by controlled IR assays in stage 3 (S3) of the screen, as described below.

Induced resistance (IR) assays

Two-week-old seedlings were grown in 60-mL pots, after which the soil was saturated with water, *(R)*-β-homoserine (Sigma-Aldrich; #03694), or R/S-BABA (Sigma-Aldrich, #A44207) to the indicated concentrations, as described previously (Buswell et al., 2018). Two days after chemical treatment, seedlings were spray-inoculated with a suspension of *Hpa* conidiospores (10^5 spores/mL) and maintained in 100% RH to promote infection. Leaves were collected at 6-7 dpi for trypan blue staining for microscopy scoring of *Hpa* colonization by categorizing them into four classes, ranging from healthy leaves (I) to heavily colonized leaves (IV), as described in detail by Schwarzenbacher et al. (2020). To investigate augmented induction of cell wall defense by chemical priming treatment, leaves were harvested at 3 dpi for aniline blue/calcofluor staining and analysis by epifluorescence microscopy (Leica DM6B; light source: CoolLED pE-2; 365 nm excitation filter, L 425 nm emission filter, 400 nm dichroic filter). For each genotype/treatment combination, germinated coniodiospores on 10 leaves from independent seedlings were scored either as arrested (spores or germ tubes fully encased in callose), or non-arrested by callose depositions (no callose or lateral callose deposition along the germ tube/hyphae), as detailed by Schwarzenbacher *et al.* (2020). Statistical differences in in *Hpa* colonization or callose defense were analyzed by pairwise Fisher's exact tests, using R software (v 3.5.1). For multiple comparisons, an additional Bonferroni multiple correction was applied, using the R package 'fifer' (fifer_1.1.tar.gz).

Plant growth assays

Surface-sterilized seeds were sown onto half-strength MS agar plates and cultivated for 2 weeks under standard plant growth conditions, as indicated above. Photographs were taken after 1 and 2 weeks of growth with a Nikon D5300 digital camera. Green leaf areas (GLA) were quantified from digital photographs of 1- or 2-week-old seedlings, using Fiji/ImageJ software (Rueden et al., 2017). Statistical differences in the natural logarithm of (1+GLA) were analyzed by two-way ANOVA, using R software (v 3.5.1).

Genotyping verification by PCR and gene expression analysis by reverse transcription quantitative PCR (RT-qPCR)

Genomic T-DNA insertions of all *iri1, iri2, iri3 and iri4* lines were confirmed by PCR using LP+RP and LBb1.3/ LB3+RP primers (Supplemental Table S2) To quantify *LHT1*

expression levels by RT-qPCR, shoot tissues from five 2-week-old seedlings were collected and combined as one biological replicate. A total of five replicates were collected at the same time and snap-frozen in liquid nitrogen and homogenized. Total RNA was extracted using an RNeasy Plant Mini Kit (Qiagen, cat. no. 74904) and first-strand cDNA was synthesized from 800 ng total RNA using a Maxima First Strand cDNA Synthesis Kit (Thermo Fisher, cat. no. K1641). The cDNA was diluted 20 times in nuclease-free water before qPCR. All qPCR reactions were performed with 2 µL diluted cDNA and primer concentrations at a final concentration of 250 nM in a Rotor-Gene Q real-time PCR cycler (Qiagen, Q-Rex v1.0), using a Rotor-Gene SYBR Green PCR Kit (Qiagen, cat. no. 204074). The qPCR amplification of *LHT1* was performed with gene-specific primers (FP: ATCTCCGGCGTTTCTCTTGCTG, RP: GCCCATGCGATTGTTGAGTAGCTG) and normalized to the transcript levels of two housekeeping genes (At1g13440 [*GLYCERALDEHYDE-3-PHOSPHATE DEHYDROGENASE C2*, *GAPC2*], and At2g28390 [*MONENSIN SENSITIVITY 1*, *MON1*]), as detailed previously (Schwarzenbacher et al., 2020).

Quantification of *in planta* RBH and BABA concentrations by hydrophilic interaction liquid chromatography coupled to quadrupole time-of-flight mass spectrometry

Shoot tissues were collected at 2 days after soil-drenching and divided into four replicate tubes per treatment (five plants per tube, from separate trays), frozen at –80°C, freeze-dried and weighed. Dry tissue was crushed and extracted into 1 mL of cold extraction buffer (methanol: water: formic acid, 10:89.99:0.01, v/v/v). Extracts were centrifuged at 16,000 g for 5 min at 4°C, after which each supernatant was divided between three aliquots. RBH and BABA standards were prepared as individual standards from 0.1 to 100 µM. Separation was performed with a Waters Acquity HILIC BEH C18 analytical column, 1.7-mm particle size, 2.1 x 50 mm. The mobile phase was 20 mM ammonium formate with 0.1% (v/v) formic acid (A) and acetonitrile with 0.1% (v/v) formic acid (B). The gradient started at 99% (v/v) A and reached 65% (v/v) A in 4 min. The gradient changed to 1% (v/v) A up to 6 min and was held there for 1.5 min and then returned to initial conditions. The solvent flow rate was 0.3 mL min^{-1}, with an injection volume of 4 µL. Mass spectra were recorded in positive electro-spray ionization mode, using a Waters UPLC system interfaced to a Waters quadrupole time-of-flight mass spectrometer (Q-TOF; G2Si Synapt). Nitrogen was used as the drying and nebulizing gas. Desolvation gas flow was adjusted to approximately 150 L/h and the cone gas flow was set to 20 L/h with a cone voltage of 5 V and a capillary voltage of 2.5 kV. The

nitrogen desolvation temperature was 280°C and the source temperature was 100°C. The instrument was calibrated in 20-1,200 m/z range with a sodium formate solution. Leucine enkephalin (Sigma-Aldrich, St. Louis MO, USA) in methanol: water (50:50, v/v) with 0.1% (v/v) formic acid was simultaneously introduced into the qTOF instrument via the lock-spray needle for recalibrating the *m/z* axis. Quantification of amino acids in tissues was based on the standard curves, using MassLynx v4.1 software (Waters, Elstree UK). Amino acids identities were confirmed by co-elution of product fragment ions with parent ions and matching peak retention times to individual amino acid standards. Statistical differences in RBH and BABA between genotypes and soil-drench treatments were tested by two-way ANOVA followed by Welch t-tests to test cross-genotype differences at each RBH/BABA concentration, using R software (v 3.5.1).

Yeast transformation

The *LHT1* (At5g40780) coding sequence with stop codon was amplified from wild-type Col-0 cDNA with Phusion High-Fidelity DNA Polymerase (New England Biolabs, #M0530L) and cloned into the pENTR plasmid (Invitrogen). *LHT1* was then subcloned into pDR196 (Meyer et al., 2006) by restriction (EcoRI and XhoI) and ligation **(**T4 DNA ligase). Empty vector (EV)- and *LHT1*-harboring plasmids were confirmed by Sanger sequencing and introduced into competent cells of the 22Δ10α strain (Besnard et al., 2016), using heat shock transformation (Gietz and Schiestl, 2007).

Yeast growth assays

To assess the growth of *LHT1*- and EV-transformed 22Δ10α yeast strains, cells were first cultivated in liquid Yeast Nitrogen Base (YNB) medium (Alfa Aesar, #H26271, without amino acids and ammonium sulfate) supplemented with 10 mM ammonium sulfate at 30℃ and 220 rpm for 2 days. Cells were washed by centrifugation at room temperature (3,000 g; 5 min) and resuspended in distilled water to an OD_{600} of 0.3-0.5. To assess whether yeast can metabolize RBH and BABA, 5 µL of the cell suspension was added to 2 mL Yeast Nitrogen Base and increasing concentrations of RBH or BABA (0.2–5 mM). To assess toxicity of RBH and BABA, 5 uL of the suspension was added to 2 mL YNB medium with 10 mM ammonium sulfate and increasing concentrations of RBH or BABA (0.2–5 mM). To assess competition between L-Ala and RBH or BABA, 5 µL of the suspension was added to 2 mL YNB medium supplemented with 1 mM L-Ala and increasing concentrations of RBH or BABA (0.2–5 mM). cultures were incubated at 30℃ with 220 rpm shaking for 3 days, after

678 which the OD_{595} was determined in a plate reader (FLUOstar OPTIMA; BMG LABTECH;
679 Germany).

680

681 **Assessment of uptake and inhibition kinetics of LHT1 in yeast**

682 Transformed 22Δ10α cells were grown in YNB medium supplemented with 10 mM
683 $(NH_4)_2SO_4$ at 30℃ with shaking at 220 rpm for 2 days. Yeast cells were collected by
684 centrifugation at room temperature (3000 g; 5 min), washed in distilled water, and
685 resuspended in ice-cold washing buffer (0.6 M sorbitol, 50 mM sodium phosphate, pH 4.5) to
686 OD_{600} of 5. Before the uptake assay, cells were energized by adding 1 M glucose (final
687 concentration 50 mM) to the growth medium for 10 min. To assess time-dependent uptake of
688 L-[^{14}C] Ala in EV- and *LHT1*-transformed cells (Supplemental Figure S8), 1.5-mL of the
689 energized cell culture was added to 1.5 mL uptake buffer, containing 50 nCi L-[^{14}C]Ala (158
690 mCi/mmol; Perkin Elmer; NEC856) with unlabeled L-Ala (50 or 500 µM). After 2, 5 or
691 10 min of incubation in a thermomixer (Grant bio ES-20; Grant Instruments; UK; 30℃,
692 220 rpm), the cell suspensions were mixed with 2 mL ice-cold water and kept on ice to
693 inhibit L-Ala uptake. Cells were then centrifuged (3000 g; 5 min; 4°C) and washed four
694 times with 2 mL ice-cold water, after which pellets were stored at –20°C for
695 quantification of radioactivity the following day. To determine uptake and inhibition
696 kinetics (Figure 6C,D), *LHT1*-transformed cells were incubated in the same uptake medium,
697 containing 50 nCi L-[^{14}C] Ala with increasing concentrations (1–3,000 µM) of unlabeled
698 L-Ala and/or 500 µM inhibitory RBH or BABA. After 5 min of incubation, cells were
699 washed, collected, and stored as described above. To assess radioactivity, frozen pellets
700 were resuspended in 750 µL distilled water, from which 200 µL was loaded onto
701 Combusto-Pads (Perkin Elmer, part number 5067034) and combusted in a sample
702 oxidizer (Model 307 Sample Oxidizer; Perkin Elmer; USA). Trapped $^{14}CO_2$ was
703 quantified by liquid scintillation counting (Tri-Carb 3100TR; Perkin Elmer; USA). L-
704 Ala uptake velocities over the 5-min time window (V_{uptake}) were expressed as fmol L-
705 Ala/cell and plotted against the L-Ala concentration, using the R package drc (Ritz et al.,
706 2015) to determine the kinetics of L-Ala uptake in the absence and presence of RBH or
707 BABA.

To estimate inhibition constants (Ki) of RBH and BABA (Figure 6E,F), L-Ala uptake velocities were determined in the presence of 0, 250 and 1,000 µM RBH or BABA, using a medium containing increasing concentrations of L-Ala (1, 5, 25, 50, 250 µM) with a fixed quantity of 50 nCi L-[^{14}C]Ala. Dixon plots were created by plotting inverse L-Ala uptake velocities ($1/V_{uptake}$) against inhibitor concentration (RBH or BABA), after which five linear models for each L-Ala concentration were generated using the *lm* function (R base). Exact Ki values of RBH and BABA were determined by modeling 1,200 $1/V_{uptake}$ values in the range between -200 to 1,000 µM of the inhibitor concentration using the *predict()* function (R base), after which Ki values were selected by calculating the inhibitor concentration yielding the minimum range in $1/V_{uptake}$.

Accession numbers

LHT1 (*IRI1*): At5g40780

Supplemental Data

Supplemental Figure S1. Validation of putative *iri* mutants at stage 3 of the mutant screen.

Supplemental Figure S2. Characterization of RBH-IR in mutants carrying independent T-DNA insertions in the annotated genes disrupted by the SALK/SAIL lines in *iri2-1*, *iri3-1* and *iri4-1*.

Supplemental Figure S3. Genetic characterization of two independent *lht1* mutant lines and the *LHT1* overexpression line.

Supplemental Figure S4. Transgenic overexpression of *LHT1* improves Arabidopsis growth on medium with L-alanine as the only N source, which is antagonized by co-application of RBH.

Supplemental Figure S5. Comparison of growth repression by low concentrations of BABA and RBH.

Supplemental Figure S6. RBH and BABA compete with L-alanine for LHT1 uptake and inhibit yeast growth.

Supplemental Figure S7. RBH and BABA have minimal effects on yeast growth but cannot be used as N source by yeast.

Supplemental Figure S8. Transformation of the yeast 22Δ10α mutant with *LHT1* rescues uptake of L-[^{14}C] alanine.

Supplemental figure S9. Modeling exact inhibitor constants (Ki) of RBH (A) and BABA.

Supplemental Figure S10. Induction of *LHT1* expression by *Hpa.*

Supplemental Table 1. Primers used for characterization of T-DNA insertion lines.

Supplemental Data Set S1. Annotated genomic T-DNA insertions of the 108 confirmed *iri* lines, RBH-IR phenotypes, and expression profiles of the associated T-DNA-tagged genes.

Supplemental Data Set S2. Details of statistical tests and results used in the manuscript.

ACKNOWLEDGEMENTS

We thank Dr. Henrik Svennerstam for providing the seeds of the *35Spro:LHT1* line, Professor Guillaume Pilot for providing the 22Δ10α yeast line, Professor Stephen Rolfe and Dr. Pedro Rocha for advice on the enzyme kinetic experiment. We thank Dr. Karin Posthuma (Enza Zaden) for advice and support throughout the project. We gratefully acknowledge PhD student support from The De Laszlo Foundation. This work was supported by a grant from the European Research Council (ERC; no. 309944 "Prime-A-Plant") to J.T., a Research Leadership Award from the Leverhulme Trust (no. RL-2012-042) to J.T., a BBSRC-IPA grant to J.T. (BB/P006698/1) and Supplementary grant from Enza Zaden to J.T., and a ERC-PoC grant to JT (no. 824985 "ChemPrime). K.F. is supported by a European Research Council Consolidator Grant (MYCOREV - 865225). The authors declare no financial conflict of interest.

AUTHOR CONTRIBUTIONS

J.T. conceived the research; C.-N.T, W.B., P.Z., R.S., and J.T. designed the experiments; C.-N.T, W.B., P.Z., H.W., I.J., and K.F. conducted the experiments; C.-N.T, W.B., P.Z., and J.T. analyzed the data; C.-N.T, W.B., and J.T. wrote the paper.

Figure legends

Figure 1. Mutant screen for *impaired in RBH-induced immunity* (*iri*) phenotypes and characterization of the *iri1* mutant in Arabidopsis.

(A) Schematic diagram of the three successive selection stages of the *iri* mutant screen on 23,547 T-DNA insertion lines from the SALK/SAIL collection. Small populations of ~five

seedlings were screened per line (stage 1) and rescreened (stage 2) for sporulation by *Hyalopoeronospora arabidopsidis* WACO9 (*Hpa*) upon saturating the soil to a final concentrations of 0.5 mM R-β-homoserine (RBH) and subsequent inoculation with *Hpa* conidionspores (top). Putative *iri* lines were validated in controlled RBH-induced resistance (RBH-IR) assays by scoring leaves from water- and RBH-treated (0.5 mM) plants into four *Hpa* colonization classes at 5-7 days post inoculation (dpi; bottom; Supplemental Figure 1). Representative photographs of trypan blue-stained leaves on the bottom left indicate the *Hpa* colonization classes, ranging from healthy leaves (I), hyphal colonization without conidiospores (II), hyphal colonization with conidiophores (III), to extensive hyphal colonization with conidiophores and deposition of sexual oospores (IV).
(B) Gene model of the *IRI1* gene (At5g40780) encoding LYSINE HISTIDINE TRANSPORTER1 (LHT1). Red triangles indicate two independent T-DNA insertions in the *lht1-5* (*iri1-1*) and *lht1-4* (*iri1-2*) mutants, respectively, to confirm the involvment of *LHT1* in RBH-IR against *Hpa.*
(**C**) Quantification of RBH-IR against *Hpa* in leaves of Col-0, *lht1-4* and *lht1-5.* Shown are frequency distributions of trypan blue-stained leaves across the four *Hpa* colonization classes (see **A**). Different letters indicate statistically significant differences between samples at 6 dpi (Fisher's exact tests + Bonferroni FDR; $p < 0.05$; n = 70-80 leaves).
(**D**) Quantification of arrested *Hpa* colonization by callose. *Hpa*-induced callose was analyzed in aniline blue/calcofluor-stained leaves by epifluorescence microscopy. Shown are percentages of callose-arrested and non-arrested conidiospores at 3 dpi, as detailed by Schwarzenbacher et al. (2020). Different letters indicate statistically significant differences in frequencies between samples (Fisher's exact tests + Bonferroni FDR; $p < 0.05$; $n > 100$ conidiospores).

Figure 2. LHT1 controls RBH-uptake and RBH-induced resistance against *Hpa*.
(A) Quantification of RBH in leaves of Col-0 (wild-type), *lht1-5 (*mutant) and *35Spro: LHT1* (overexpression) plants after soaking the soil to saturation with increasing RBH concentrations. Leaves were collected at 2 days after soil treatment with RBH and analyzed by HILIC-Q-TOF. Boxplots show median (middle bar), interquartile range (IQR; box), 1.5 x IQR (whiskers) and replication units (single dots) of leaf RBH concentrations (nmol/g dry weight [DW]). Inset shows *p*-values of statistically significant effects on RBH concentration by genotype, soil treatment and their interaction (two-way ANOVA). Asterisks indicate statistically significant differences relative to Col-0 for each soil treatment (Welch t-test; **, $p<0.01$; *, $0.01<p<0.05$).
(B) Quantification of RBH-induced resistance against *Hpa* Col-0, *lht1-5* and *35Spro:LHT1*. Two-week-old seedlings had the soil of their pots saturated with increasing concentrations of RBH and challenge-inoculated with *Hpa* conidiospores 2 days later. Shown are frequency distributions of trypan blue-stained leaves across four *Hpa* colonization classes at 6 dpi (see Figure 1A). Different letters indicate statistically significant differences between samples (Fisher's exact tests + Bonferroni FDR; $p < 0.05$; n = 70-90 leaves).

Figure 3. Overexpression of *LHT1* renders Arabidopsis susceptible to growth repression by RBH, which is antagonized by co-application of L-alanine
(A) *LHT1*-dependent effects of RBH and L-alanine on plant growth. Shown are 2-week-old seedlings of Col-0 (upper left), *lht1-5* (upper right), and *35Spro: LHT1* (bottom) grown on MS agar plates, supplemented with 10 mM $(NH_4)_2SO_4$ and increasing concentrations of RBH and/or L-alanine.
(B) Quantification of green leaf area (GLA ± SEM; n=7-19) in 1-week-old Col-0, *lht1-5,* and *35Spro:LHT1* seedlings from the same experiment. Inset shows *p*-values of effects on GLA

by RBH concentration, L-alanine concentration and their interaction inside each genotype (two-way ANOVA).

Figure 4. LHT1 controls BABA-uptake and BABA-induced resistance against *Hpa*

(A) Quantification of BABA in leaves of Col-0 (wild-type) and *lht1-5* (mutant) plants after soaking the soil to saturation with increasing BABA concentrations. Leaves were collected at 2 days after soil treatment and analyzed by HILIC-Q-TOF. Boxplots show median (middle bar), interquartile range (IQR; box), 1.5 x IQR (whiskers) and replication units (single dots) of leaf BABA concentrations (nmol/g DW). Inset shows *p*-values of statistically significant effects on BABA concentration by genotype, soil treatment and their interaction (two-way ANOVA). Asterisks indicate statistically significant differences to Col-0 for each soil treatment (Welch t-test; **, $p<0.01$; *, $0.01<p<0.05$).

(B) Quantification of BABA-induced resistance against *Hpa* in Col-0, *lht1-5* and *35Spro:LHT1* seedlings. Two-week-old seedlings had the soil of their pots saturated with increasing concentrations of BABA and challenge-inoculated with *Hpa* conidiospores 2 days later. Shown are frequency distributions of trypan blue-stained leaves across four *Hpa* colonization classes at 6 dpi (see Figure **1A**). Different letters indicate statistically significant differences between samples (Fisher's exact tests + Bonferroni FDR; $p < 0.05$; n = 70-80 leaves).

Figure 5. LHT1 controls stress tolerance to BABA

(A) Effects of BABA on growth by Col-0, *lht1-5, 35Spro:LHT1* Shown are 2-week-old seedlings of Col-0 (upper left), *lht1-5* (upper right), and *35Spro:LHT1* (bottom) grown on MS agar plates, supplemented with increasing concentrations of BABA.

(B) Average green leaf areas (GLA ± SEM; n=14-20) of 1-week-old Col-0, *lht1-5*, *35Spro:LHT1* plants from the same experiment. Asterisks indicate statistically significant differences compared to Col-0 at each BABA concentration (Welch t-tests + Bonferroni FDR; $p < 0.05$).

Figure 6. Characterization of RBH and BABA uptake kinetics by LHT1 via heterologous expression in yeast

(A, B) Transformation of the yeast mutant 22Δ10α (Besnard et al., 2016) with Arabidopsis *LHT1* rescues growth on agar (**A**) or liquid medium (**B**) with L-alanine (L-Ala) as the only nitrogen source. Shown in (A) are growth phenotypes of empty vector (EV)- and *LHT1*-transformed 22Δ10α cells on agar medium supplemented with inorganic nitrogen (10 mM $(NH_4)_2SO_4$; top) or 1 mM L-alanine (bottom). (B) Growth of EV- and *LHT1*-transformed 22Δ10α in liquid medium supplemented with increasing L-Ala concentrations. Data points and lines represent individual measurements and means of ΔOD595 values (n=4), respectively.

(C, D) Competitive inhibition of LHT1-dependent uptake of L-Ala by RBH (**C**; blue) and BABA (**D**; red). Uptake velocities by LHT1 were determined in the presence of increasing L-Ala concentrations containing 50 nCi ^{14}C-labeled L-Ala with and without 500 µM RBH (C) or BABA (D). Data points represent L-Ala uptake velocities (fmol L-Ala/cell; n=3) over a 5-min time window. In the absence of RBH or BABA, the Km for L-Ala-uptake by LHT1 was 9.4 µM. Competitive inhibition by RBH and BABA is shown by a decrease in Km but not Vmax.

(E, F) Dixon plots to determine the inhibition constants (Ki) of RBH (**E**) and BABA (**F**). Ki values were determined in the presence of increasing L-Ala concentrations containing a fixed amount of 50 nCi ^{14}C-labeled L-Ala and 0, 250 and 1,000 µM of RBH or BABA. Data points represent values of inverse L-Ala uptake velocities over a 5-min time window (cell/fmol L-

Ala; n=3). Dotted vertical lines indicate intercepts at Ki values of RBH and BABA (see also Supplemental Figure S9).

REFERENCES

Ahmad, S., Gordon-Weeks, R., Pickett, J., and Ton, J. (2010). Natural variation in priming of basal resistance: from evolutionary origin to agricultural exploitation. Molecular Plant Pathology 11, 817-827.

Alonso, J.M., and Ecker, J.R. (2006). Moving forward in reverse: genetic technologies to enable genome-wide phenomic screens in Arabidopsis. Nature Reviews Genetics 7, 524-536.

Badmi, R., Zhang, Y., Tengs, T., Brurberg, M.B., Krokene, P., Fossdal, C.G., Hytönen, T., and Thorstensen, T. (2019). Induced and primed defense responses of *Fragaria vesca* to *Botrytis cinerea* infection. bioRxiv, 692491.

Balmer, A., Glauser, G., Mauch-Mani, B., and Baccelli, I. (2019). Accumulation patterns of endogenous beta-aminobutyric acid during plant development and defense in *Arabidopsis thaliana*. Plant Biology 21, 318-325.

Besnard, J., Pratelli, R., Zhao, C., Sonawala, U., Collakova, E., Pilot, G., and Okumoto, S. (2016). UMAMIT14 is an amino acid exporter involved in phloem unloading in Arabidopsis roots. Journal of experimental botany 67, 6385-6397.

Bigeard, J., Colcombet, J., and Hirt, H. (2015). Signaling mechanisms in pattern-triggered immunity (PTI). Mol Plant 8, 521-539.

Boorer, K.J., Frommer, W.B., Bush, D.R., Kreman, M., Loo, D.D.F., and Wright, E.M. (1996). Kinetics and specificity of a H+ amino acid transporter from *Arabidopsis thaliana*. Journal of Biological Chemistry 271, 2213-2220.

Buswell, W., Schwarzenbacher, R.E., Luna, E., Sellwood, M., Chen, B., Flors, V., Pétriacq, P., and Ton, J. (2018). Chemical priming of immunity without costs to plant growth. New Phytologist 218, 1205-1216.

Camanes, G., Pastor, V., Cerezo, M., Garcia-Andrade, J., Vicedo, B., Garcia-Agustin, P., and Flors, V. (2012). A Deletion in NRT2.1 Attenuates *Pseudomonas syringae*-induced hormonal perturbation, resulting in primed plant defenses. Plant Physiology 158, 1054-1066.

Cameron, D.D., Neal, A.L., van Wees, S.C.M., and Ton, J. (2013). Mycorrhiza-induced resistance: more than the sum of its parts? Trends in Plant Science 18, 539-545.

Chen, L., and Bush, D.R. (1997). LHT1, a lysine-and histidine-specific amino acid transporter in Arabidopsis. Plant Physiology 115, 1127-1134.

Chen, Y., Yan, Y., Ren, Z.-F., Ganeteg, U., Yao, G.-K., Li, Z.-L., Huang, T., Li, J.-H., Tian, Y.-Q., Lin, F., and Xu, H.-H. (2018). AtLHT1 Transporter can facilitate the uptake and translocation of a Glycinergic-Chlorantraniliprole conjugate in *Arabidopsis thaliana*. Journal of Agricultural and Food Chemistry 66, 12527-12535.

Chisholm, S.T., Coaker, G., Day, B., and Staskawicz, B.J. (2006). Host-microbe interactions: shaping the evolution of the plant immune response. Cell 124, 803-814.

Choi, H.W., and Klessig, D.F. (2016). DAMPs, MAMPs, and NAMPs in plant innate immunity. BMC plant biology 16, 1-10.

Choi, J., Eom, S., Shin, K., Lee, R.-A., Choi, S., Lee, J.-H., Lee, S., and Soh, M.-S. (2019). Identification of Lysine Histidine Transporter 2 as an 1-Aminocyclopropane

915 Carboxylic Acid Transporter in Arabidopsis thaliana by Transgenic Complementation
916 Approach. Frontiers in plant science 10, 1092-1092.
917 Cohen, Y. (1994). 3-Aminobutyric acid induces systemic resistance against *Peronospore*
918 *tabacina*. Physiological and Molecular Plant Pathology 44, 273-288.
919 Cohen, Y., Vaknin, M., and Mauch-Mani, B. (2016). BABA-induced resistance: milestones
920 along a 55-year journey. Phytoparasitica 44, 513-538.
921 Cornish-Bowden, A. (1974). A simple graphical method for determining the inhibition
922 constants of mixed, uncompetitive and non-competitive inhibitors (Short
923 Communication). Biochemical Journal: Molecular Aspects 137, 143-144.
924 Cui, H., Tsuda, K., and Parker, J.E. (2015). Effector-triggered immunity: from pathogen
925 perception to robust defense. Annu Rev Plant Biol 66, 487-511.
926 De Kesel, J., Conrath, U., Flors, V., Luna, E., Mageroy, M.H., Mauch-Mani, B., Pastor, V.,
927 Pozo, M.J., Pieterse, C.M., and Ton, J. (2021). The induced resistance lexicon: Do's
928 and don'ts. Trends in Plant Science
929 De Muyt, A., Pereira, L., Vezon, D., Chelysheva, L., Gendrot, G., Chambon, A., Lainé-
930 Choinard, S., Pelletier, G., Mercier, R., and Nogué, F. (2009). A high throughput
931 genetic screen identifies new early meiotic recombination functions in *Arabidopsis*
932 *thaliana*. PLoS genetics 5, e1000654.
933 Dinkeloo, K., Boyd, S., and Pilot, G. (2018). Update on amino acid transporter functions and
934 on possible amino acid sensing mechanisms in plants. In Seminars in cell &
935 developmental biology (Elsevier), pp. 105-113.
936 Dobritsa, A.A., Geanconteri, A., Shrestha, J., Carlson, A., Kooyers, N., Coerper, D.,
937 Urbanczyk-Wochniak, E., Bench, B.J., Sumner, L.W., and Swanson, R. (2011). A
938 large-scale genetic screen in Arabidopsis to identify genes involved in pollen exine
939 production. Plant Physiology 157, 947-970.
940 Elashry, A., Okumoto, S., Siddique, S., Koch, W., Kreil, D.P., and Bohlmann, H. (2013). The
941 AAP gene family for amino acid permeases contributes to development of the cyst
942 nematode *Heterodera schachtii* in roots of Arabidopsis. Plant Physiology
943 Biochemistry 70, 379-386.
944 Gelvin, S.B. (2021). Plant DNA Repair and Agrobacterium T-DNA Integration. International
945 Journal of Molecular Sciences 22.
946 Gietz, R.D., and Schiestl, R.H. (2007). High-efficiency yeast transformation using the
947 LiAc/SS carrier DNA/PEG method. Nature Protocols 2, 31-34.
948 Guether, M., Volpe, V., Balestrini, R., Requena, N., Wipf, D., and Bonfante, P. (2011).
949 LjLHT1.2-a mycorrhiza-inducible plant amino acid transporter from *Lotus japonicus*.
950 Biology and Fertility of Soils 47, 925-936.
951 Hirner, A., Ladwig, F., Stransky, H., Okumoto, S., Keinath, M., Harms, A., Frommer, W.B.,
952 and Koch, W. (2006). Arabidopsis LHT1 is a high-affinity transporter for cellular
953 amino acid uptake in both root epidermis and leaf mesophyll. The Plant Cell 18,
954 1931-1946.
955 Ho, C.-H., Lin, S.-H., Hu, H.-C., and Tsay, Y.-F. (2009). CHL1 functions as a nitrate sensor
956 in plants. Cell 138, 1184-1194.
957 Jiang, X., Xie, Y., Ren, Z., Ganeteg, U., Lin, F., Zhao, C., and Xu, H. (2018). Design of a
958 new Glutamine-Fipronil conjugate with alpha-amino acid function and its uptake by
959 A-thaliana Lysine Histidine Transporter 1 (AtLHT1). Journal of Agricultural and
960 Food Chemistry 66, 7597-7605.
961 Khare, D., Choi, H., Huh, S.U., Bassin, B., Kim, J., Martinoia, E., Sohn, K.H., Paek, K.-H.,
962 and Lee, Y.J.P.o.t.N.A.o.s. (2017). Arabidopsis ABCG34 contributes to defense

against necrotrophic pathogens by mediating the secretion of camalexin. Proceedings of the National Academy of Sciences of the United States of America 114, E5712-E5720.

Kus, J.V., Zaton, K., Sarkar, R., and Cameron, R.K. (2002). Age-related resistance in Arabidopsis is a developmentally regulated defense response to *Pseudomonas syringae*. Plant Cell 14, 479-490.

Liu, G., Ji, Y., Bhuiyan, N.H., Pilot, G., Selvaraj, G., Zou, J., and Wei, Y. (2010). Amino acid homeostasis modulates salicylic acid–associated redox status and defense responses in Arabidopsis. The Plant Cell 22, 3845-3863.

Lu, X., Dittgen, J., Piślewska-Bednarek, M., Molina, A., Schneider, B., Svato¡, A., Doubský, J., Schneeberger, K., Weigel, D., and Bednarek, P. (2015). Mutant allele-specific uncoupling of PENETRATION3 functions reveals engagement of the ATP-binding cassette transporter in distinct tryptophan metabolic pathways. Plant Physiology 168, 814-827.

Luna, E., Van Hulten, M., Zhang, Y., Berkowitz, O., López, A., Pétriacq, P., Sellwood, M.A., Chen, B., Burrell, M., and Van De Meene, A. (2014). Plant perception of β-aminobutyric acid is mediated by an aspartyl-tRNA synthetase. Nature chemical biology 10, 450-456.

Marella, H.H., Nielsen, E., Schachtman, D.P., and Taylor, C.G. (2013). The Amino Acid Permeases AAP3 and AAP6 are involved in root-knot nematode parasitism of Arabidopsis. Molecular Plant-Microbe Interactions 26, 44-54.

Mauch-Mani, B., Baccelli, I., Luna, E., and Flors, V. (2017). Defense priming: an adaptive part of induced resistance. Annual review of plant biology 68, 485-512.

Meyer, A., Eskandari, S., Grallath, S., and Rentsch, D. (2006). AtGAT1, a high affinity transporter for γ-aminobutyric acid in Arabidopsis thaliana. Journal of biological chemistry 281, 7197-7204.

O'Malley, R.C., Barragan, C.C., and Ecker, J.R. (2015). A user's guide to the Arabidopsis T-DNA insertion mutant collections. In Plant Functional Genomics (Springer), pp. 323-342.

Ritz, C., Baty, F., Streibig, J.C., and Gerhard, D. (2015). Dose-response analysis using R. PLoS One 10, e0146021-e0146021.

Rueden, C.T., Schindelin, J., Hiner, M.C., DeZonia, B.E., Walter, A.E., Arena, E.T., and Eliceiri, K.W. (2017). ImageJ2: ImageJ for the next generation of scientific image data. Bmc Bioinformatics 18.

Schwarzenbacher, R.E., Wardell, G., Stassen, J., Guest, E., Zhang, P., Luna, E., and Ton, J. (2020). The IBI1 receptor of β-aminobutyric acid interacts with VOZ transcription factors to regulate abscisic acid signaling and callose-associated defense. Molecular plant 13, 1455-1469.

Serrano, M., Wang, B., Aryal, B., Garcion, C., Abou-Mansour, E., Heck, S., Geisler, M., Mauch, F., Nawrath, C., and Métraux, J.-P. (2013). Export of salicylic acid from the chloroplast requires the multidrug and toxin extrusion-like transporter EDS5. Plant physiology 162, 1815-1821.

Shin, K., Lee, S., Song, W.-Y., Lee, R.-A., Lee, I., Ha, K., Koo, J.-C., Park, S.-K., Nam, H.-G., and Lee, Y. (2015). Genetic identification of ACC-RESISTANT2 reveals involvement of LYSINE HISTIDINE TRANSPORTER1 in the uptake of 1-aminocyclopropane-1-carboxylic acid in Arabidopsis thaliana. Plant Cell Physiology 56, 572-582.

Sonawala, U., Dinkeloo, K., Danna, C.H., McDowell, J.M., and Pilot, G. (2018). Review: Functional linkages between amino acid transporters and plant responses to pathogens. Plant Science 277, 79-88.

Svennerstam, H., Ganeteg, U., Bellini, C., and Nasholm, T. (2007). Comprehensive screening of Arabidopsis mutants suggests the lysine histidine transporter 1 to be involved in plant uptake of amino acids. Plant Physiology 143, 1853-1860.

Svennerstam, H., Jamtgard, S., Ahmad, I., Huss-Danell, K., Nasholm, T., and Ganeteg, U. (2011). Transporters in Arabidopsis roots mediating uptake of amino acids at naturally occurring concentrations. New Phytol 191, 459-467.

Thevenet, D., Pastor, V., Baccelli, I., Balmer, A., Vallat, A., Neier, R., Glauser, G., and Mauch-Mani, B. (2017). The priming molecule β-aminobutyric acid is naturally present in plants and is induced by stress. New Phytologist 213, 552-559.

Ton, J., Jakab, G., Toquin, V., Flors, V., Iavicoli, A., Maeder, M.N., Métraux, J.-P., and Mauch-Mani, B. (2005). Dissecting the β-aminobutyric acid–induced priming phenomenon in Arabidopsis. The Plant Cell 17, 987-999.

Wilkinson, S.W., Mageroy, M.H., Lopez Sanchez, A., Smith, L.M., Furci, L., Cotton, T.E.A., Krokene, P., and Ton, J. (2019). Surviving in a hostile world: plant strategies to resist pests and diseases. Annu Rev Phytopathol 57, 505-529.

Wilson-Sánchez, D., Rubio-Díaz, S., Muñoz-Viana, R., Pérez-Pérez, J.M., Jover-Gil, S., Ponce, M.R., and Micol, J.L. (2014). Leaf phenomics: a systematic reverse genetic screen for Arabidopsis leaf mutants. The Plant Journal 79, 878-891.

Wu, C.-C., Singh, P., Chen, M.-C., and Zimmerli, L. (2010). L-Glutamine inhibits beta-aminobutyric acid-induced stress resistance and priming in Arabidopsis. Journal of experimental botany 61, 995-1002.

Yang, H., Bogner, M., Stierhof, Y.-D., and Ludewig, U. (2010). H+-Independent glutamine transport in plant root tips. Plos One 5.

Yang, H., Postel, S., Kemmerling, B., and Ludewig, U. (2014). Altered growth and improved resistance of Arabidopsis against *Pseudomonas syringae* by overexpression of the basic amino acid transporter AtCAT1. Plant, cell environment 37, 1404-1414.

Yassin, M., Ton, J., Rolfe, S.A., Valentine, T.A., Cromey, M., Holden, N., and Newton, A.C. (2021). The rise, fall and resurrection of chemical-induced resistance agents. Pest Management Science 77, 3900-3909.

Yoshino, M., and Murakami, K. (2009). A graphical method for determining inhibition constants. Journal of Enzyme Inhibition and Medicinal Chemistry 24, 1288-1290

Yoo, H., Greene, G.H., Yuan, M., Xu, G., Burton, D., Liu, L., Marques, J., and Dong, X. (2020). Translational Regulation of Metabolic Dynamics during Effector-Triggered Immunity. Mol Plant 13, 88-98.

Zhang, X., Khadka, P., Puchalski, P., Leehan, J.D., Rossi, F.R., Okumoto, S., Pilot, G., and Danna, C.H. (2022). MAMP-elicited changes in amino acid transport activity contribute to restricting bacterial growth. Plant Physiol

Zimmerli, L., Jakab, G., Métraux, J.-P., and Mauch-Mani, B. (2000). Potentiation of pathogen-specific defense mechanisms in Arabidopsis by β-aminobutyric acid. Proceedings of the National Academy of Sciences 97, 12920-12925.

1055

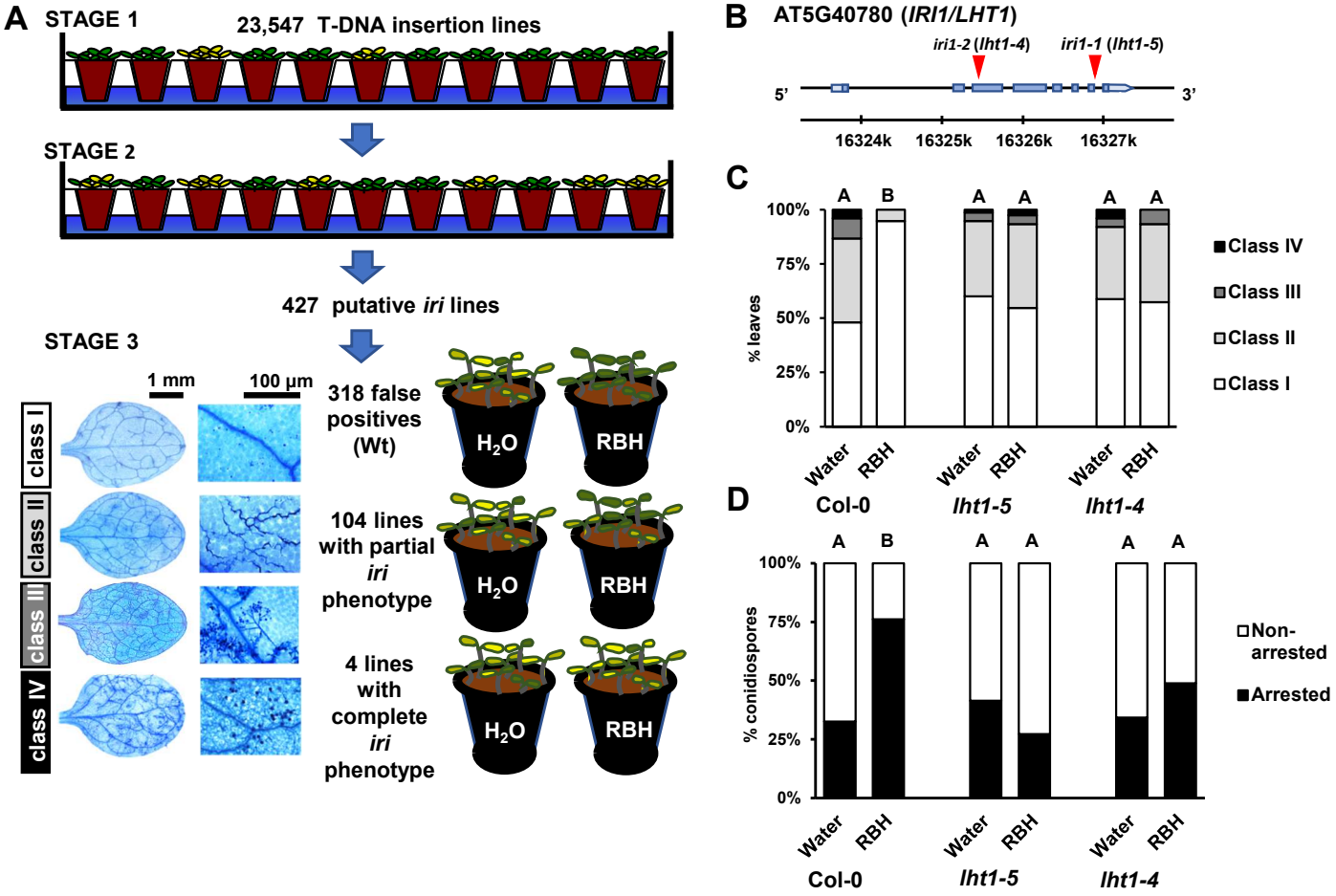

Figure 1. Mutant screen for *impaired in RBH-induced immunity* (*iri*) phenotypes and characterization of the *iri1* mutant in Arabidopsis.

(A) Schematic diagram of the three successive selection stages of the *iri* mutant screen on 23,547 T-DNA insertion lines from the SALK/SAIL collection. Small populations of ~five seedlings were screened per line (stage 1) and rescreened (stage 2) for sporulation by *Hyalopoeronospora arabidopsidis* WACO9 (*Hpa*) upon saturating the soil to a final concentrations of 0.5 mM R-β-homoserine (RBH) and subsequent inoculation with *Hpa* conidionspores (top). Putative *iri* lines were validated in controlled RBH-induced resistance (RBH-IR) assays by scoring leaves from water- and RBH-treated (0.5 mM) plants into four *Hpa* colonization classes at 5-7 days post inoculation (dpi; bottom; Supplemental Figure 1). Representative photographs of trypan blue-stained leaves on the bottom left indicate the *Hpa* colonization classes, ranging from healthy leaves (I), hyphal colonization without conidiospores (II), hyphal colonization with conidiophores (III), to extensive hyphal colonization with conidiophores and deposition of sexual oospores (IV).

(B) Gene model of the *IRI1* gene (At5g40780) encoding LYSINE HISTIDINE TRANSPORTER1 (LHT1). Red triangles indicate two independent T-DNA insertions in the *lht1-5* (*iri1-1*) and *lht1-4* (*iri1-2*) mutants, respectively, to confirm the involvment of *LHT1* in RBH-IR against *Hpa.*

(**C**) Quantification of RBH-IR against *Hpa* in leaves of Col-0, *lht1-4* and *lht1-5.* Shown are frequency distributions of trypan blue-stained leaves across the four *Hpa* colonization classes (see **A**). Different letters indicate statistically significant differences between samples at 6 dpi (Fisher's exact tests + Bonferroni FDR; $p < 0.05$; n = 70-80 leaves).

(**D**) Quantification of arrested *Hpa* colonization by callose. *Hpa*-induced callose was analyzed in aniline blue/calcofluor-stained leaves by epifluorescence microscopy. Shown are percentages of callose-arrested and non-arrested conidiospores at 3 dpi, as detailed by Schwarzenbacher et al. (2020). Different letters indicate statistically significant differences in frequencies between samples (Fisher's exact tests + Bonferroni FDR; $p < 0.05$; $n > 100$ conidiospores).

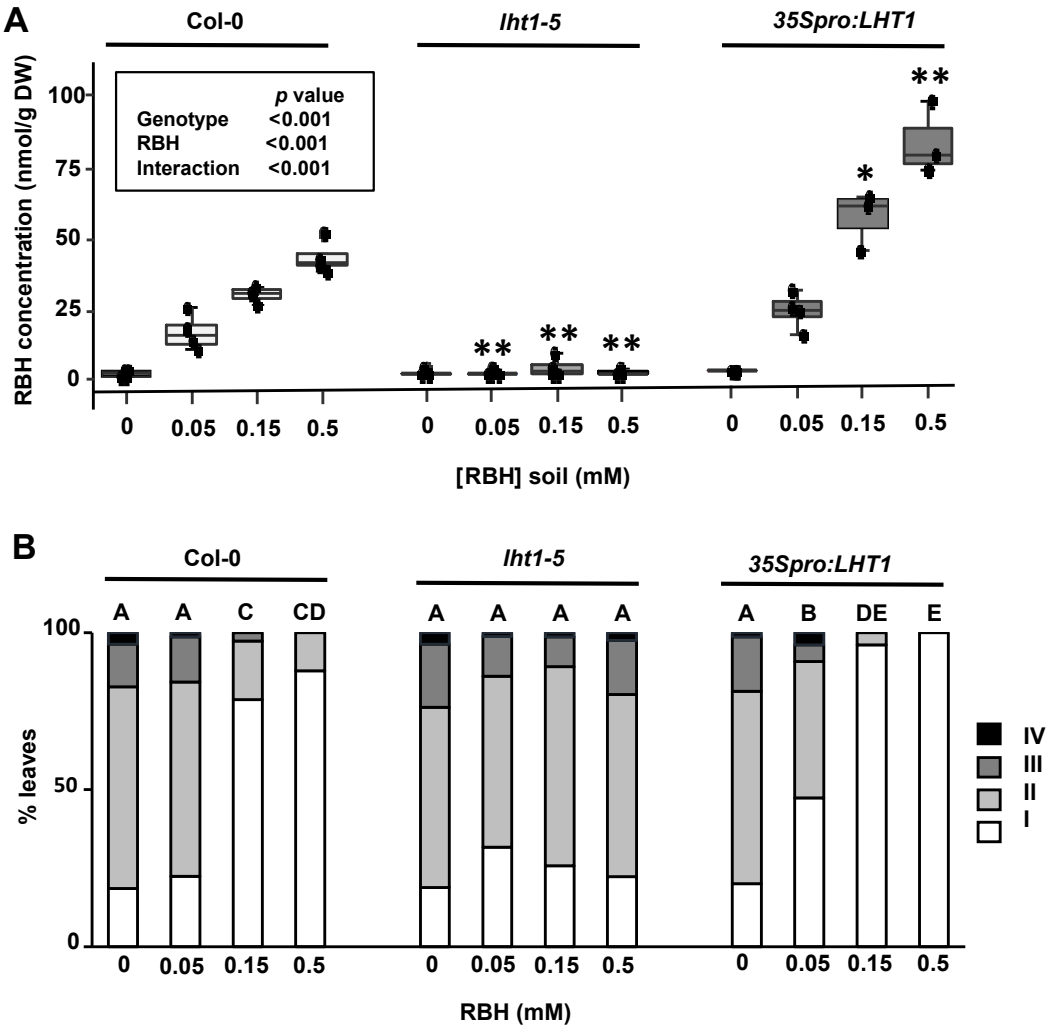

Figure 2. LHT1 controls RBH-uptake and RBH-induced resistance against *Hpa*.

(A) Quantification of RBH in leaves of Col-0 (wild-type), *lht1-5 (*mutant) and *35Spro: LHT1* (overexpression) plants after soaking the soil to saturation with increasing RBH concentrations. Leaves were collected at 2 days after soil treatment with RBH and analyzed by HILIC-Q-TOF. Boxplots show median (middle bar), interquartile range (IQR; box), 1.5 x IQR (whiskers) and replication units (single dots) of leaf RBH concentrations (nmol/g dry weight [DW]). Inset shows *p*-values of statistically significant effects on RBH concentration by genotype, soil treatment and their interaction (two-way ANOVA). Asterisks indicate statistically significant differences relative to Col-0 for each soil treatment (Welch t-test; **, $p<0.01$; *, $0.01<p<0.05$).

(B) Quantification of RBH-induced resistance against *Hpa* Col-0, *lht1-5* and *35Spro:LHT1*. Two-week-old seedlings had the soil of their pots saturated with increasing concentrations of RBH and challenge-inoculated with *Hpa* conidiospores 2 days later. Shown are frequency distributions of trypan blue-stained leaves across four *Hpa* colonization classes at 6 dpi (see Figure 1A). Different letters indicate statistically significant differences between samples (Fisher's exact tests + Bonferroni FDR; $p < 0.05$; n = 70-90 leaves).

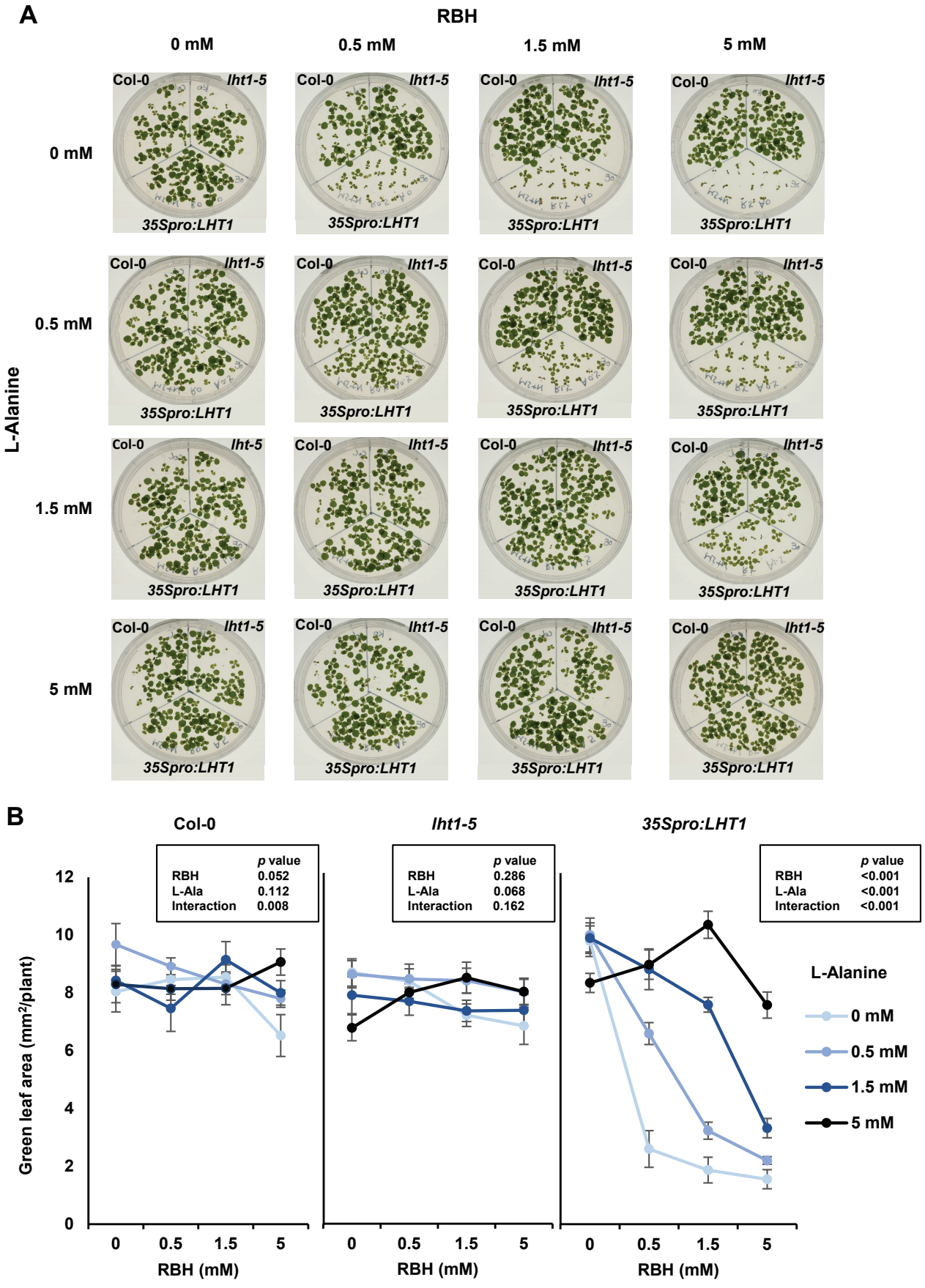

Figure 3. Overexpression of *LHT1* renders Arabidopsis susceptible to growth repression by RBH, which is antagonized by co-application of L-alanine

(A) *LHT1*-dependent effects of RBH and L-alanine on plant growth. Shown are 2-week-old seedlings of Col-0 (upper left), *lht1-5* (upper right), and *35Spro: LHT1* (bottom) grown on MS agar plates, supplemented with 10 mM $(NH_4)_2SO_4$ and increasing concentrations of RBH and/or L-alanine.

(B) Quantification of green leaf area (GLA ± SEM; n=7-19) in 1-week-old Col-0, *lht1-5,* and *35Spro:LHT1* seedlings from the same experiment. Inset shows *p*-values of effects on GLA by RBH concentration, L-alanine concentration and their interaction inside each genotype (two-way ANOVA).

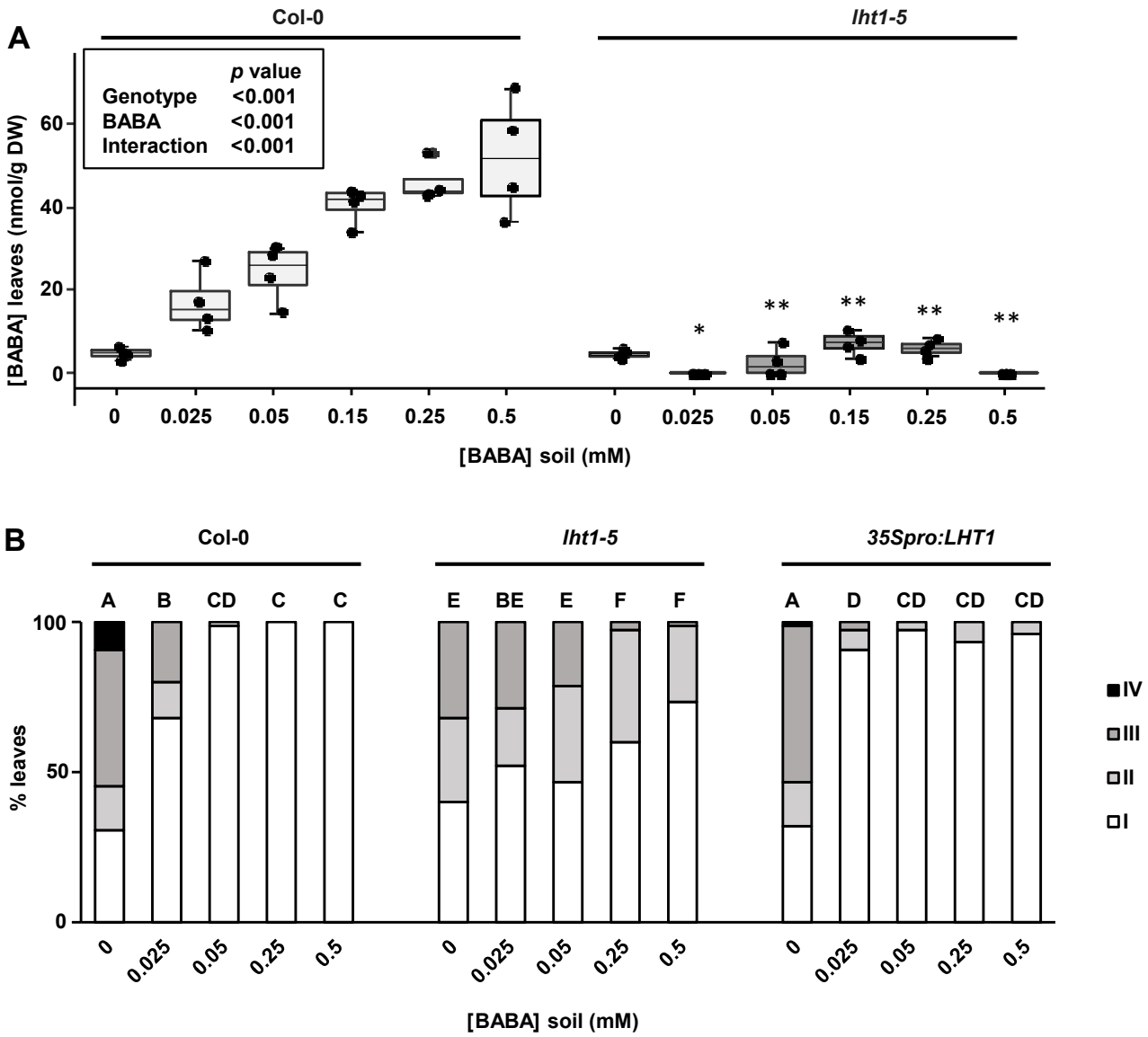

Figure 4. LHT1 controls BABA-uptake and BABA-induced resistance against *Hpa*

(A) Quantification of BABA in leaves of Col-0 (wild-type) and *lht1-5* (mutant) plants after soaking the soil to saturation with increasing BABA concentrations. Leaves were collected at 2 days after soil treatment and analyzed by HILIC-Q-TOF. Boxplots show median (middle bar), interquartile range (IQR; box), 1.5 x IQR (whiskers) and replication units (single dots) of leaf BABA concentrations (nmol/g DW). Inset shows *p*-values of statistically significant effects on BABA concentration by genotype, soil treatment and their interaction (two-way ANOVA). Asterisks indicate statistically significant differences to Col-0 for each soil treatment (Welch t-test; **, $p<0.01$; *, $0.01<p<0.05$).

(B) Quantification of BABA-induced resistance against *Hpa* in Col-0, *lht1-5* and *35Spro:LHT1* seedlings. Two-week-old seedlings had the soil of their pots saturated with increasing concentrations of BABA and challenge-inoculated with *Hpa* conidiospores 2 days later. Shown are frequency distributions of trypan blue-stained leaves across four *Hpa* colonization classes at 6 dpi (see Figure **1A**). Different letters indicate statistically significant differences between samples (Fisher's exact tests + Bonferroni FDR; $p < 0.05$; n = 70-80 leaves).

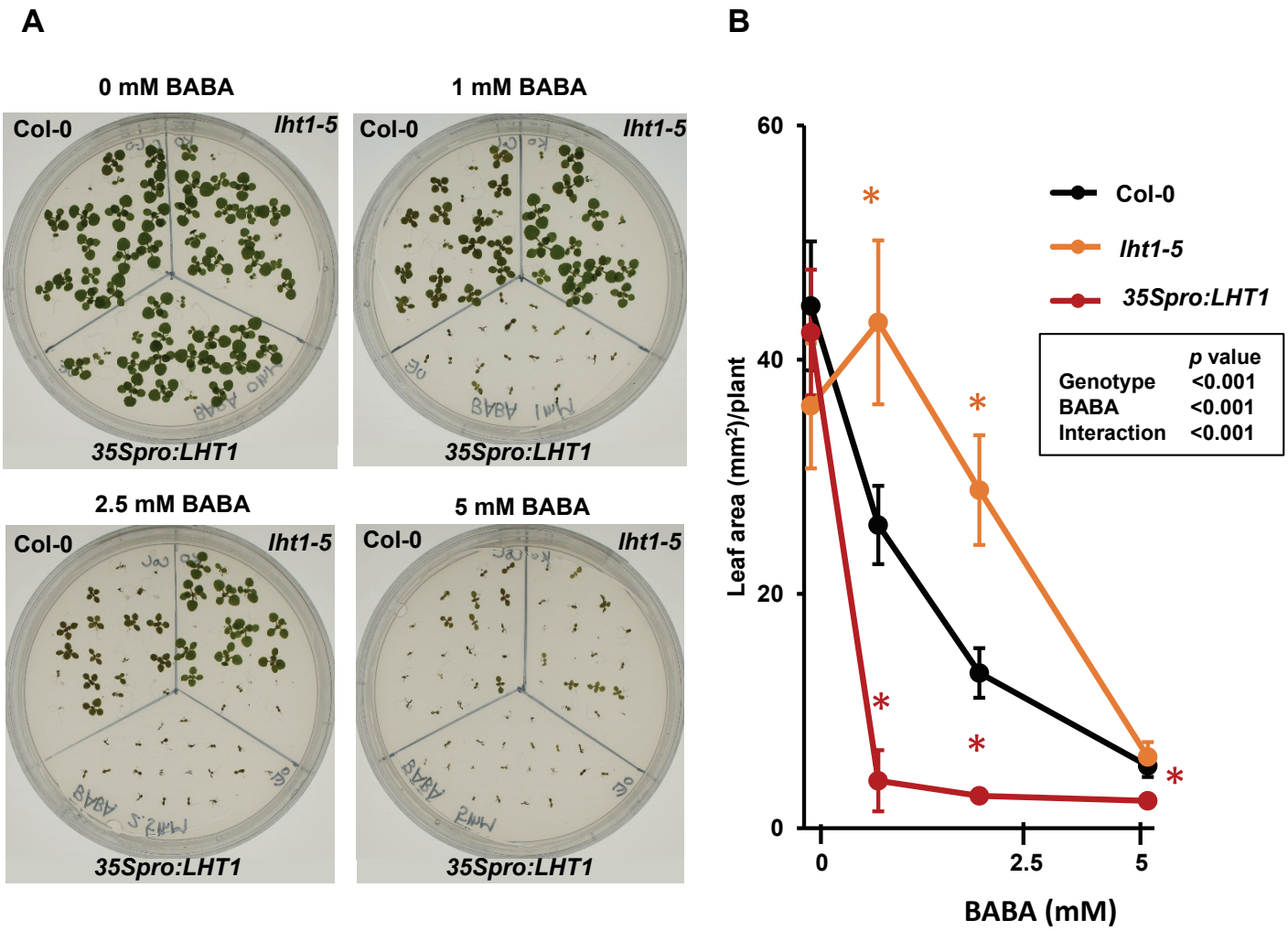

Figure 5. LHT1 controls stress tolerance to BABA

(A) Effects of BABA on growth by Col-0, *lht1-5, 35Spro:LHT1* Shown are 2-week-old seedlings of Col-0 (upper left), *lht1-5* (upper right), and *35Spro:LHT1* (bottom) grown on MS agar plates, supplemented with increasing concentrations of BABA.

(B) Average green leaf areas (GLA ± SEM; n=14-20) of 1-week-old Col-0, *lht1-5*, *35Spro:LHT1* plants from the same experiment. Asterisks indicate statistically significant differences compared to Col-0 at each BABA concentration (Welch t-tests + Bonferroni FDR; $p < 0.05$).

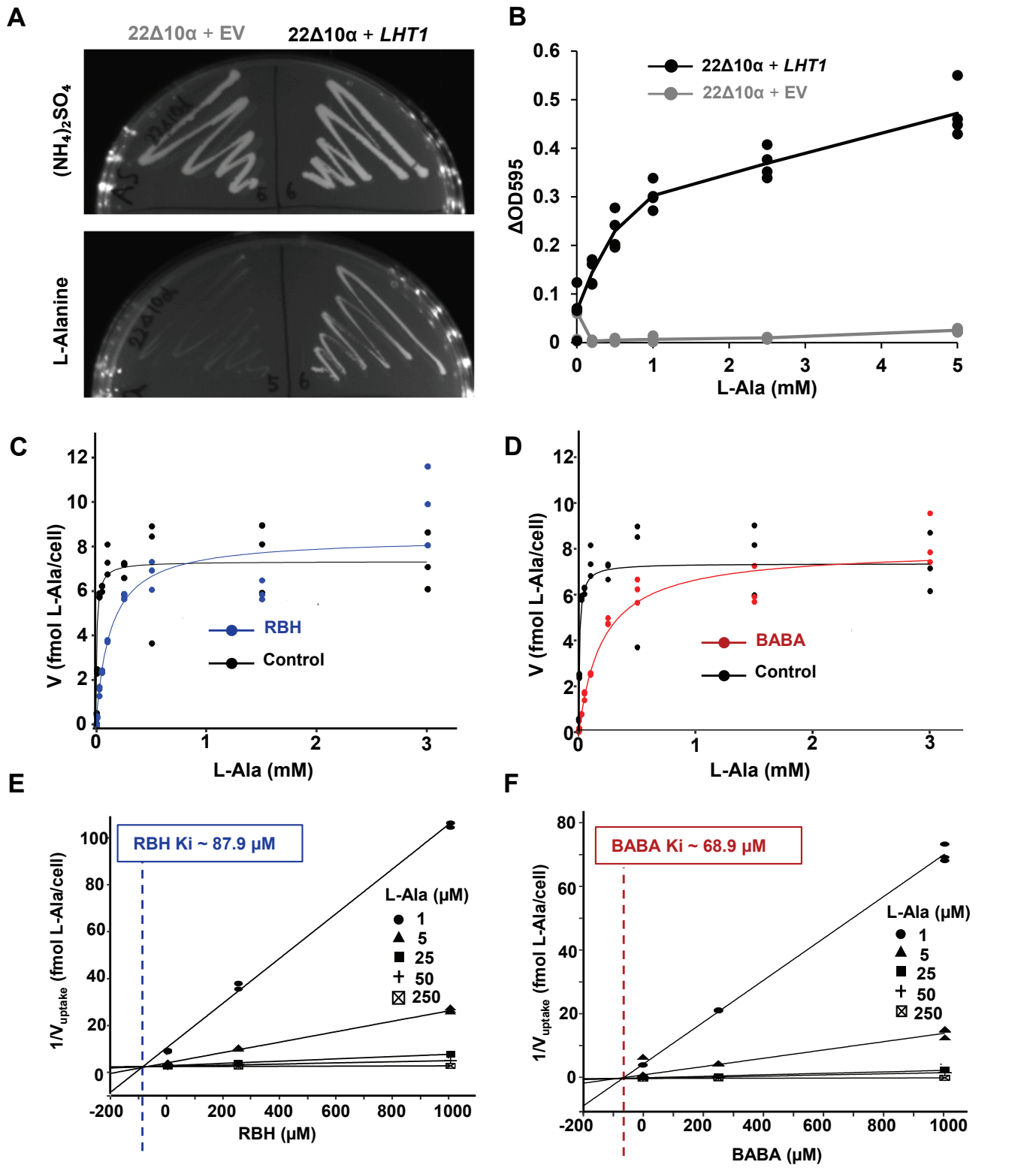

Figure 6. Characterization of RBH and BABA uptake kinetics by LHT1 via heterologous expression in yeast

(A, B) Transformation of the yeast mutant 22Δ10α (Besnard et al., 2016) with Arabidopsis *LHT1* rescues growth on agar (**A**) or liquid medium (**B**) with L-alanine (L-Ala) as the only nitrogen source. Shown in (A) are growth phenotypes of empty vector (EV)- and *LHT1*-transformed 22Δ10α cells on agar medium supplemented with inorganic nitrogen (10 mM $(NH_4)_2SO_4$; top) or 1 mM L-alanine (bottom). (B) Growth of EV- and *LHT1*-transformed 22Δ10α in liquid medium supplemented with increasing L-Ala concentrations. Data points and lines represent individual measurements and means of ΔOD595 values (n=4), respectively.

(C, D) Competitive inhibition of LHT1-dependent uptake of L-Ala by RBH (**C**; blue) and BABA (**D**; red). Uptake velocities by LHT1 were determined in the presence of increasing L-Ala concentrations containing 50 nCi ^{14}C-labeled L-Ala with and without 500 μM RBH (C) or BABA (D). Data points represent average L-Ala uptake velocities (fmol L-Ala/cell; n=3) over a 5-min time window. In the absence of RBH or BABA, the Km for L-Ala-uptake by LHT1 was 9.4 μM. Competitive inhibition by RBH and BABA is shown by a decrease in Km but not Vmax.

(E, F) Dixon plots to determine the inhibition constants (Ki) of RBH (**E**) and BABA (**F**). Ki values were determined in the presence of increasing L-Ala concentrations containing a fixed amount of 50 nCi ^{14}C-labeled L-Ala and 0, 250 and 1,000 μM of RBH or BABA. Data points represent mean values of inverse L-Ala uptake velocities over a 5-min time window (cell/fmol L-Ala; n=3). Dotted vertical lines indicate intercepts at Ki values of RBH and BABA (see also Supplemental Figure S9).

Parsed Citations

Ahmad, S., Gordon-Weeks, R., Pickett, J., and Ton, J. (2010). Natural variation in priming of basal resistance: from evolutionary origin to agricultural exploitation. Molecular Plant Pathology 11, 817-827.
Google Scholar: Author Only Title Only Author and Title

Alonso, J.M., and Ecker, J.R. (2006). Moving forward in reverse: genetic technologies to enable genome-wide phenomic screens in Arabidopsis. Nature Reviews Genetics 7, 524-536.
Google Scholar: Author Only Title Only Author and Title

Badmi, R., Zhang, Y., Tengs, T., Brurberg, M.B., Krokene, P., Fossdal, C.G., Hytönen, T., and Thorstensen, T. (2019). Induced and primed defense responses of Fragaria vesca to Botrytis cinerea infection. bioRxiv, 692491.
Google Scholar: Author Only Title Only Author and Title

Balmer, A., Glauser, G., Mauch-Mani, B., and Baccelli, I. (2019). Accumulation patterns of endogenous beta-aminobutyric acid during plant development and defense in Arabidopsis thaliana. Plant Biology 21, 318-325.
Google Scholar: Author Only Title Only Author and Title

Besnard, J., Pratelli, R., Zhao, C., Sonawala, U., Collakova, E., Pilot, G., and Okumoto, S. (2016). UMAMIT14 is an amino acid exporter involved in phloem unloading in Arabidopsis roots. Journal of experimental botany 67, 6385-6397.
Google Scholar: Author Only Title Only Author and Title

Bigeard, J., Colcombet, J., and Hirt, H. (2015). Signaling mechanisms in pattern-triggered immunity (PTI). Mol Plant 8, 521-539.
Google Scholar: Author Only Title Only Author and Title

Boorer, K.J., Frommer, W.B., Bush, D.R., Kreman, M., Loo, D.D.F., and Wright, E.M. (1996). Kinetics and specificity of a H+ amino acid transporter from Arabidopsis thaliana. Journal of Biological Chemistry 271, 2213-2220.
Google Scholar: Author Only Title Only Author and Title

Buswell, W., Schwarzenbacher, R.E., Luna, E., Sellwood, M., Chen, B., Flors, V., Pétriacq, P., and Ton, J. (2018). Chemical priming of immunity without costs to plant growth. New Phytologist 218, 1205-1216.
Google Scholar: Author Only Title Only Author and Title

Camanes, G., Pastor, V., Cerezo, M., Garcia-Andrade, J., Vicedo, B., Garcia-Agustin, P., and Flors, V. (2012). A Deletion in NRT2.1 Attenuates Pseudomonas syringae-induced hormonal perturbation, resulting in primed plant defenses. Plant Physiology 158, 1054-1066.
Google Scholar: Author Only Title Only Author and Title

Cameron, D.D., Neal, A.L., van Wees, S.C.M., and Ton, J. (2013). Mycorrhiza-induced resistance: more than the sum of its parts? Trends in Plant Science 18, 539-545.
Google Scholar: Author Only Title Only Author and Title

Chen, L., and Bush, D.R. (1997). LHT1, a lysine-and histidine-specific amino acid transporter in Arabidopsis. Plant Physiology 115, 1127-1134.
Google Scholar: Author Only Title Only Author and Title

Chen, Y., Yan, Y., Ren, Z.-F., Ganeteg, U., Yao, G.-K., Li, Z.-L., Huang, T., Li, J.-H., Tian, Y.-Q., Lin, F., and Xu, H.-H. (2018). AtLHT1 Transporter can facilitate the uptake and translocation of a Glycinergic-Chlorantraniliprole conjugate in Arabidopsis thaliana. Journal of Agricultural and Food Chemistry 66, 12527-12535.
Google Scholar: Author Only Title Only Author and Title

Chisholm, S.T., Coaker, G., Day, B., and Staskawicz, B.J. (2006). Host-microbe interactions: shaping the evolution of the plant immune response. Cell 124, 803-814.
Google Scholar: Author Only Title Only Author and Title

Choi, H.W., and Klessig, D.F. (2016). DAMPs, MAMPs, and NAMPs in plant innate immunity. BMC plant biology 16, 1-10.
Google Scholar: Author Only Title Only Author and Title

Choi, J., Eom, S., Shin, K., Lee, R.-A., Choi, S., Lee, J.-H., Lee, S., and Soh, M.-S. (2019). Identification of Lysine Histidine Transporter 2 as an 1-Aminocyclopropane Carboxylic Acid Transporter in Arabidopsis thaliana by Transgenic Complementation Approach. Frontiers in plant science 10, 1092-1092.
Google Scholar: Author Only Title Only Author and Title

Cohen, Y. (1994). 3-Aminobutyric acid induces systemic resistance against Peronospore tabacina. Physiological and Molecular Plant Pathology 44, 273-288.
Google Scholar: Author Only Title Only Author and Title

Cohen, Y., Vaknin, M., and Mauch-Mani, B. (2016). BABA-induced resistance: milestones along a 55-year journey. Phytoparasitica 44, 513-538.
Google Scholar: Author Only Title Only Author and Title

Cornish-Bowden, A. (1974). A simple graphical method for determining the inhibition constants of mixed, uncompetitive and non-competitive inhibitors (Short Communication). Biochemical Journal: Molecular Aspects 137, 143-144.
Google Scholar: Author Only Title Only Author and Title

Cui, H., Tsuda, K., and Parker, J.E. (2015). Effector-triggered immunity: from pathogen perception to robust defense. Annu Rev Plant Biol 66, 487-511.
Google Scholar: Author Only Title Only Author and Title

De Kesel, J., Conrath, U., Flors, V., Luna, E., Mageroy, M.H., Mauch-Mani, B., Pastor, V., Pozo, M.J., Pieterse, C.M., and Ton, J. (2021). The induced resistance lexicon: Do's and don'ts. Trends in Plant Science
Google Scholar: Author Only Title Only Author and Title

De Muyt, A., Pereira, L., Vezon, D., Chelysheva, L., Gendrot, G., Chambon, A., Lainé-Choinard, S., Pelletier, G., Mercier, R., and Nogué, F. (2009). A high throughput genetic screen identifies new early meiotic recombination functions in Arabidopsis thaliana. PLoS genetics 5, e1000654.
Google Scholar: Author Only Title Only Author and Title

Dinkeloo, K., Boyd, S., and Pilot, G. (2018). Update on amino acid transporter functions and on possible amino acid sensing mechanisms in plants. In Seminars in cell & developmental biology (Elsevier), pp. 105-113.
Google Scholar: Author Only Title Only Author and Title

Dobritsa, A.A., Geanconteri, A., Shrestha, J., Carlson, A., Kooyers, N., Coerper, D., Urbanczyk-Wochniak, E., Bench, B.J., Sumner, L.W., and Swanson, R. (2011). A large-scale genetic screen in Arabidopsis to identify genes involved in pollen exine production. Plant Physiology 157, 947-970.
Google Scholar: Author Only Title Only Author and Title

Elashry, A., Okumoto, S., Siddique, S., Koch, W., Kreil, D.P., and Bohlmann, H. (2013). The AAP gene family for amino acid permeases contributes to development of the cyst nematode Heterodera schachtii in roots of Arabidopsis. Plant Physiology Biochemistry 70, 379-386.
Google Scholar: Author Only Title Only Author and Title

Gelvin, S.B. (2021). Plant DNA Repair and Agrobacterium T-DNA Integration. International Journal of Molecular Sciences 22.
Google Scholar: Author Only Title Only Author and Title

Gietz, R.D., and Schiestl, R.H. (2007). High-efficiency yeast transformation using the LiAc/SS carrier DNA/PEG method. Nature Protocols 2, 31-34.
Google Scholar: Author Only Title Only Author and Title

Guether, M., Volpe, V., Balestrini, R., Requena, N., Wipf, D., and Bonfante, P. (2011). LjLHT1.2-a mycorrhiza-inducible plant amino acid transporter from Lotus japonicus. Biology and Fertility of Soils 47, 925-936.
Google Scholar: Author Only Title Only Author and Title

Hirner, A., Ladwig, F., Stransky, H., Okumoto, S., Keinath, M., Harms, A., Frommer, W.B., and Koch, W. (2006). Arabidopsis LHT1 is a high-affinity transporter for cellular amino acid uptake in both root epidermis and leaf mesophyll. The Plant Cell 18, 1931-1946.
Google Scholar: Author Only Title Only Author and Title

Ho, C.-H., Lin, S.-H., Hu, H.-C., and Tsay, Y.-F. (2009). CHL1 functions as a nitrate sensor in plants. Cell 138, 1184-1194.
Google Scholar: Author Only Title Only Author and Title

Jiang, X., Xie, Y., Ren, Z., Ganeteg, U., Lin, F., Zhao, C., and Xu, H. (2018). Design of a new Glutamine-Fipronil conjugate with alpha-amino acid function and its uptake by A-thaliana Lysine Histidine Transporter 1 (AtLHT1). Journal of Agricultural and Food Chemistry 66, 7597-7605.
Google Scholar: Author Only Title Only Author and Title

Khare, D., Choi, H., Huh, S.U., Bassin, B., Kim, J., Martinoia, E., Sohn, K.H., Paek, K.-H., and Lee, Y.J.P.o.t.N.A.o.s. (2017). Arabidopsis ABCG34 contributes to defense against necrotrophic pathogens by mediating the secretion of camalexin. Proceedings of the National Academy of Sciences of the United States of America 114, E5712-E5720.
Google Scholar: Author Only Title Only Author and Title

Kus, J.V., Zaton, K., Sarkar, R., and Cameron, R.K. (2002). Age-related resistance in Arabidopsis is a developmentally regulated defense response to Pseudomonas syringae. Plant Cell 14, 479-490.
Google Scholar: Author Only Title Only Author and Title

Liu, G., Ji, Y., Bhuiyan, N.H., Pilot, G., Selvaraj, G., Zou, J., and Wei, Y. (2010). Amino acid homeostasis modulates salicylic acid–associated redox status and defense responses in Arabidopsis. The Plant Cell 22, 3845-3863.
Google Scholar: Author Only Title Only Author and Title

Lu, X., Dittgen, J., Piślewska-Bednarek, M., Molina, A., Schneider, B., Svato¡, A., Doubský, J., Schneeberger, K., Weigel, D., and Bednarek, P. (2015). Mutant allele-specific uncoupling of PENETRATION3 functions reveals engagement of the ATP-binding cassette transporter in distinct tryptophan metabolic pathways. Plant Physiology 168, 814-827.

Google Scholar: Author Only Title Only Author and Title

Luna, E., Van Hulten, M., Zhang, Y., Berkowitz, O., López, A., Pétriacq, P., Sellwood, M.A., Chen, B., Burrell, M., and Van De Meene, A. (2014). Plant perception of β-aminobutyric acid is mediated by an aspartyl-tRNA synthetase. Nature chemical biology 10, 450-456.
Google Scholar: Author Only Title Only Author and Title

Marella, H.H., Nielsen, E., Schachtman, D.P., and Taylor, C.G. (2013). The Amino Acid Permeases AAP3 and AAP6 are involved in root-knot nematode parasitism of Arabidopsis. Molecular Plant-Microbe Interactions 26, 44-54.
Google Scholar: Author Only Title Only Author and Title

Mauch-Mani, B., Baccelli, I., Luna, E., and Flors, V. (2017). Defense priming: an adaptive part of induced resistance. Annual review of plant biology 68, 485-512.
Google Scholar: Author Only Title Only Author and Title

Meyer, A., Eskandari, S., Grallath, S., and Rentsch, D. (2006). AtGAT1, a high affinity transporter for γ-aminobutyric acid in Arabidopsis thaliana. Journal of biological chemistry 281, 7197-7204.
Google Scholar: Author Only Title Only Author and Title

O'Malley, R.C., Barragan, C.C., and Ecker, J.R. (2015). A user's guide to the Arabidopsis T-DNA insertion mutant collections. In Plant Functional Genomics (Springer), pp. 323-342.
Google Scholar: Author Only Title Only Author and Title

Ritz, C., Baty, F., Streibig, J.C., and Gerhard, D. (2015). Dose-response analysis using R. PLoS One 10, e0146021-e0146021.
Google Scholar: Author Only Title Only Author and Title

Rueden, C.T., Schindelin, J., Hiner, M.C., DeZonia, B.E., Walter, A.E., Arena, E.T., and Eliceiri, K.W. (2017). ImageJ2: ImageJ for the next generation of scientific image data. Bmc Bioinformatics 18.
Google Scholar: Author Only Title Only Author and Title

Schwarzenbacher, R.E., Wardell, G., Stassen, J., Guest, E., Zhang, P., Luna, E., and Ton, J. (2020). The IBI1 receptor of β-aminobutyric acid interacts with VOZ transcription factors to regulate abscisic acid signaling and callose-associated defense. Molecular plant 13, 1455-1469.
Google Scholar: Author Only Title Only Author and Title

Serrano, M., Wang, B., Aryal, B., Garcion, C., Abou-Mansour, E., Heck, S., Geisler, M., Mauch, F., Nawrath, C., and Métraux, J.-P. (2013). Export of salicylic acid from the chloroplast requires the multidrug and toxin extrusion-like transporter EDS5. Plant physiology 162, 1815-1821.
Google Scholar: Author Only Title Only Author and Title

Shin, K., Lee, S., Song, W.-Y., Lee, R.-A., Lee, I., Ha, K., Koo, J.-C., Park, S.-K., Nam, H.-G., and Lee, Y. (2015). Genetic identification of ACC-RESISTANT2 reveals involvement of LYSINE HISTIDINE TRANSPORTER1 in the uptake of 1-aminocyclopropane-1-carboxylic acid in Arabidopsis thaliana. Plant Cell Physiology 56, 572-582.
Google Scholar: Author Only Title Only Author and Title

Sonawala, U., Dinkeloo, K., Danna, C.H., McDowell, J.M., and Pilot, G. (2018). Review: Functional linkages between amino acid transporters and plant responses to pathogens. Plant Science 277, 79-88.
Google Scholar: Author Only Title Only Author and Title

Svennerstam, H., Ganeteg, U., Bellini, C., and Nasholm, T. (2007). Comprehensive screening of Arabidopsis mutants suggests the lysine histidine transporter 1 to be involved in plant uptake of amino acids. Plant Physiology 143, 1853-1860.
Google Scholar: Author Only Title Only Author and Title

Svennerstam, H., Jamtgard, S., Ahmad, I., Huss-Danell, K., Nasholm, T., and Ganeteg, U. (2011). Transporters in Arabidopsis roots mediating uptake of amino acids at naturally occurring concentrations. New Phytol 191, 459-467.
Google Scholar: Author Only Title Only Author and Title

Thevenet, D., Pastor, V., Baccelli, I., Balmer, A., Vallat, A., Neier, R., Glauser, G., and Mauch-Mani, B. (2017). The priming molecule β-aminobutyric acid is naturally present in plants and is induced by stress. New Phytologist 213, 552-559.
Google Scholar: Author Only Title Only Author and Title

Ton, J., Jakab, G., Toquin, V., Flors, V., Iavicoli, A., Maeder, M.N., Métraux, J.-P., and Mauch-Mani, B. (2005). Dissecting the β-aminobutyric acid–induced priming phenomenon in Arabidopsis. The Plant Cell 17, 987-999.
Google Scholar: Author Only Title Only Author and Title

Wilkinson, S.W., Mageroy, M.H., Lopez Sanchez, A., Smith, L.M., Furci, L., Cotton, T.E.A., Krokene, P., and Ton, J. (2019). Surviving in a hostile world: plant strategies to resist pests and diseases. Annu Rev Phytopathol 57, 505-529.
Google Scholar: Author Only Title Only Author and Title

Wilson-Sánchez, D., Rubio-Díaz, S., Muñoz-Viana, R., Pérez-Pérez, J.M., Jover-Gil, S., Ponce, M.R., and Micol, J.L. (2014). Leaf phenomics: a systematic reverse genetic screen for Arabidopsis leaf mutants. The Plant Journal 79, 878-891.

Google Scholar: Author Only Title Only Author and Title

Wu, C.-C., Singh, P., Chen, M.-C., and Zimmerli, L. (2010). L-Glutamine inhibits beta-aminobutyric acid-induced stress resistance and priming in Arabidopsis. Journal of experimental botany 61, 995-1002.
Google Scholar: Author Only Title Only Author and Title

Yang, H., Bogner, M., Stierhof, Y.-D., and Ludewig, U. (2010). H+-Independent glutamine transport in plant root tips. Plos One 5.
Google Scholar: Author Only Title Only Author and Title

Yang, H., Postel, S., Kemmerling, B., and Ludewig, U. (2014). Altered growth and improved resistance of Arabidopsis against Pseudomonas syringae by overexpression of the basic amino acid transporter AtCAT1. Plant, cell environment 37, 1404-1414.
Google Scholar: Author Only Title Only Author and Title

Yassin, M., Ton, J., Rolfe, S.A., Valentine, T.A., Cromey, M., Holden, N., and Newton, A.C. (2021). The rise, fall and resurrection of chemical-induced resistance agents. Pest Management Science 77, 3900-3909.
Google Scholar: Author Only Title Only Author and Title

Yoshino, M., and Murakami, K. (2009). A graphical method for determining inhibition constants. Journal of Enzyme Inhibition and Medicinal Chemistry 24, 1288-1290
Google Scholar: Author Only Title Only Author and Title

Yoo, H., Greene, G.H., Yuan, M., Xu, G., Burton, D., Liu, L., Marques, J., and Dong, X. (2020). Translational Regulation of Metabolic Dynamics during Effector-Triggered Immunity. Mol Plant 13, 88-98.
Google Scholar: Author Only Title Only Author and Title

Zhang, X., Khadka, P., Puchalski, P., Leehan, J.D., Rossi, F.R., Okumoto, S., Pilot, G., and Danna, C.H. (2022). MAMP-elicited changes in amino acid transport activity contribute to restricting bacterial growth. Plant Physiol
Google Scholar: Author Only Title Only Author and Title

Zimmerli, L., Jakab, G., Métraux, J.-P., and Mauch-Mani, B. (2000). Potentiation of pathogen-specific defense mechanisms in Arabidopsis by β-aminobutyric acid. Proceedings of the National Academy of Sciences 97, 12920-12925.
Google Scholar: Author Only Title Only Author and Title